

SIMVASTATIN LOADED POROUS HYDROXYAPATITE BASED  
MICROCARRIERS FOR BONE TISSUE ENGINEERING

A THESIS SUBMITTED TO  
THE GRADUATE SCHOOL OF NATURAL AND APPLIED SCIENCES  
OF  
MIDDLE EAST TECHNICAL UNIVERSITY

BY

MERVE GÜLDİKEN

IN PARTIAL FULFILLMENT OF THE REQUIREMENTS  
FOR  
THE DEGREE OF MASTER OF SCIENCE  
IN  
BIOTECHNOLOGY

DECEMBER 2014



Approval of the thesis:

**SIMVASTATIN LOADED POROUS HYDROXYAPATITE BASED  
MICROCARRIERS FOR BONE TISSUE ENGINEERING**

submitted by **MERVE GÜLDİKEN** in partial fulfillment of the requirements for the degree of **Master of Science in Biotechnology Department, Middle East Technical University** by,

Prof. Dr. Gülbin Dural Ünver  
Dean, Graduate School of **Natural and Applied Sciences**

\_\_\_\_\_

Prof. Dr. Filiz Bengü Dilek  
Head of Department, **Biotechnology**

\_\_\_\_\_

Assoc. Prof. Dr. Ayşen Tezcaner  
Supervisor, **Engineering Sciences Dept., METU**

\_\_\_\_\_

Prof. Dr. Caner Durucan  
Co-Supervisor, **Metallurgical and Materials Eng. Dept., METU**

\_\_\_\_\_

**Examining Committee Members:**

Assoc. Prof. Dr. Dilek Keskin  
Engineering Sciences Dept., METU

\_\_\_\_\_

Assoc. Prof. Dr. Ayşen Tezcaner  
Engineering Sciences Dept., METU

\_\_\_\_\_

Prof. Dr. Caner Durucan  
Metallurgical and Materials Engineering Dept., METU

\_\_\_\_\_

Assoc. Prof. Dr. Erkan Türker Baran  
Center of Excellence in Biomaterials in Tissue Eng., METU

\_\_\_\_\_

Dr. Özge Erdemli  
LCPME, CNRS/Lorraine University

\_\_\_\_\_

**Date:** 29.12.2014

**I hereby declare that all information in this document has been obtained and presented in accordance with academic rules and ethical conduct. I also declare that, as required by these rules and conduct, I have fully cited and referenced all material and results that are not original to this work.**

Last name, Name: Gldiken, Merve

Signature :

## **ABSTRACT**

### **SIMVASTATIN LOADED POROUS HYDROXYAPATITE BASED MICROCARRIERS FOR BONE TISSUE ENGINEERING**

Güldiken, Merve

M.S., Department of Biotechnology

Supervisor: Assoc. Prof. Dr. Ayşen Tezcaner

Co-Supervisor: Prof. Dr. Caner Durucan

December 2014, 85 pages

Bone tissue engineering provides a new medical therapy as an alternative to conventional bone replacement grafts. Carriers designed for bone tissue engineering applications should be biocompatible, bioactive, and porous and should also meet certain minimal requirements to obtain functional engineered tissues. Polymers, ceramic materials and their composites are widely used for developing such carriers. The objective of this study was to develop and characterize a simvastatin (SIM) loaded porous hydroxyapatite microcarrier system by water in oil emulsion method for bone tissue engineering applications. In order to obtain spherical and structurally stable microcarriers, powder size should be submicron with a narrow size range. For this purpose, firstly, HAp powders (~10-17  $\mu\text{m}$ ) were synthesized using co-precipitation and sol-gel methods. It was found that powder characteristics synthesized by both methods were not suitable to form porous microcarriers. Therefore, the microcarriers were then prepared using Nano-HAp powders (<200nm). Spherical shaped and structurally stable microcarriers were obtained with

Nano-HAp powders. The average size of microcarriers prepared by Nano-HAp was determined to be 426  $\mu\text{m}$ .

The fabricated microcarriers were loaded with SIM and also coated with human decellularized adipose tissue (DAT). DAT coated and SIM loaded microcarriers were used for enhancing attachment, proliferation and osteoblastic differentiation of cells as well as for controlling SIM release. Drug loadings results were 59%, 61% and 32%, for different concentrations of SIM (1, 0.5 and 0.1 mg/ml), respectively. Release kinetics of drug loaded microcarriers could not be determined because of poor water solubility of SIM (13  $\mu\text{g/ml}$  in  $\text{dH}_2\text{O}$ ). *In vitro* cell viability of SIM loaded and DAT coated microcarriers were conducted by using PrestoBlue assay with two different cell types, Saos-2 and human adipose derived stem cells (hASCs) for 10 days. The results showed that although the loaded SIM amounts were higher than the toxic dose, microcarriers were not cytotoxic on both cell types. A higher cell attachment on DAT coated microcarriers was observed compared to un-coated microcarriers. A time dependent increase in cell number was observed on both coated and DAT un-coated microcarriers. Therefore, it can be concluded that both DAT coated and uncoated SIM loaded HA microcarriers have a potential in treating bone defects with tissue engineering applications.

**Keywords:** Bone Tissue Engineering, microcarriers, hydroxyapatite, simvastatin

## ÖZ

# KEMİK DOKU MÜHENDİSLİĞİ UYGULAMALARINA YÖNELİK SİMVASTATİN YÜKLÜ GÖZENEKLİ HİDROKSİAPATİT TEMELLİ MİKROTAŞIYICILAR

Güldiken, Merve

Yüksek Lisans, Biyoteknoloji Bölümü

Tez Yöneticisi: Doç. Dr. Ayşen Tezcaner

Ortak Tez Yöneticisi: Prof. Dr. Caner Durucan

Aralık 2014, 85 Sayfa

Kemik doku mühendisliği günümüzde uygulanmakta olan transplantasyon tedavi tekniklerine yeni bir alternatif sağlamaktadır. Biyouyumluluk, biyoaktivite, gözeneklilik ve önemli mekanik ve fiziksel gereklilikler kemik doku mühendisliği için tasarlanmış olan taşıyıcıların fonksiyonel olabilmesi için sahip olması gereken önemli özelliklerdir. Bu özellikler polimer, biyoseramik ve kompozit materyallerin kullanılması ile sağlanabilir. Bu gerekliliklerden yola çıkarak, bu çalışmadan simvastatin yüklü, hidroksiapatit temelli gözenekli mikrotasıyıcıların yağ içinde su emülsiyon yöntemi ile üretimi ve kemik doku mühendisliği alanında kullanımı için amaçlamıştır. HAp tozlarından üretilen bu taşıyıcılar için tozların parçacık boyutu oldukça önemlidir. Mikrotasıyıcıların hazırlanmasında, stabilitesini koruyan küre şeklinde bir yapı elde edebilmek için tozların parçacık boyutunun mikrondan düşük ve homojen olması gerekmektedir. Bu amaçla yola çıkarak ilk olarak ko-presipitasyon ve sol-jel adı verilen 2 farklı yöntem ile HAp tozları elde edilmiştir.

Ancak üretilen tozların boyutları gözenekli ve küresel bir mikrot taşıyıcı üretmek için uygun olmadığı görülmüştür. Bu nedenle, mikrot taşıyıcıların üretiminde Nano-HAp tozları kullanılmıştır. Elde edilen taşıyıcıların boyutları 426 µm olarak ölçülmüştür. Üretilen taşıyıcılara simvastatin yüklenmesinin ardından, yüklenen ilacın hızlı salımını engellemek, kemik dönüşümünü indüklemek ve hücrelere ekstrasellüler matris ortamı sağlayabilmek amacı ile desellülerize adipoz doku ile kaplanmıştır. Sonuçlara bakıldığında küresel şekile sahip, yapısal olarak daha dayanıklı mikrot taşıyıcılar Nano-HAp kullanılarak elde edilmiştir. Taşıyıcılara ilaç yüklenmesi, 1, 0.5 ve 0.1 mg/mL olmak üzere üç farklı ilaç konsantrasyonlarında denenmiştir ve sırasıyla ilaç yükleme verimlilikleri %59, %61 ve %32 olarak bulunmuştur. İlaç yüklenmiş mikrot taşıyıcıların salım kinetikleri simvastatinin su içerisinde çözünürlüğünün düşük olması nedeniyle belirlenememiştir. *In vitro* hücre canlılık testi ilaç yüklenmiş DAT kaplı ve kaplı olmayanlar üzerinde prestoBlue analizi kullanılarak 10 gün süre ile yapılmıştır. Bu deney için Osteosarcoma (Saos-2) hücre hattı ve adipoz kökenli kök hücreler kullanılmıştır. Elde edilen sonuçlara göre, 10 günlük inkübasyon sırasında mikrokürelere toksik SIM dozları yüklenmiş olmasına rağmen, hücreler üzerinde bu toksik etki gözlenmemiştir. Bu sonucun hazırlanan taşıyıcıların ilaç salımını yavaşlatarak daha kontrollü bir salım kinetiği oluşturduğu düşünülmektedir. Hücre ekildikten sonra yapılan SEM analizi sonrasında ise DAT kaplı mikrokürelere hücrelerin yapışan hücre sayısının daha fazla olduğu gözlemlenmiştir. Zamana bağlı hücre artışı hem DAT kaplı hem de kaplı olmayan mikrot taşıyıcılarda gözlenmiştir. Sonuç olarak DAT kaplı ve kaplanmamış olan SIM yüklenmiş HAp temelli mikrot taşıyıcıların doku mühendisliği uygulamalarında kemik hasarlarının tedavi edilmesinde bir potansiyele sahiptir.

**Anahtar Kelimeler:** Kemik doku mühendisliği, mikrot taşıyıcılar, hidroksiapatit, simvastatin

*To my Family,*

## ACKNOWLEDGMENTS

First and foremost, I am eternally grateful to my supervisor Assoc. Prof. Ayşen Tezcaner for her continuous guidance, advice, encouragement and support throughout my study. It has been an honor and an invaluable experience being her student. Her faith in me throughout my studies and her support during tough times greatly helped me to get this degree.

I owe my deepest thanks to my co-advisor Prof. Dr. Caner Durucan for his continuous support, guidance, encouragement and providing me all facilities in his Lab.

I wish to express my heartfelt gratitude to Assoc. Prof. Dilek Keskin for her guidance and all time support in my thesis study. I would also like to thank her for providing me a different point of view during my studies which helped me to resolve problems.

I also want to thank Assoc. Prof. Can Özen, for providing Laser Scanning Confocal Microscope system and offering us suggestions about our project.

I would like to express my sincere gratitude to Assoc. Prof. Zafer Evis for providing me funding during part of my studies. More importantly, I am very thankful to him for giving me the opportunity to work in his TUBITAK project which assisted me in my academic career and improved my scientific skills.

I wish to thank to BIOMATEN for allowing me to use their laboratory and Dr. Arda Büyüksungur for conducting my micro-CT analysis.

I sincerely thank one of my committee members, Assoc. Prof. Erkan Türker Baran for his contributions with his invaluable advice and spending time to improve my thesis.

I am very grateful to work with Dr. Özge Erdemli for many insightful conversations during the development of the ideas in this thesis, for helpful comments on the text for helping me get through the difficult times, and for all the emotional support.

I wish to thank Gözde Alkan for her close friendship and intellectual support that she provided me during my studies. Also, I want to thank Barış Alkan; he always creates time for my SEM and FTIR analyses.

I also want to thank M. Tümerkan Kesim for being there for me through all the good and bad times. His continuous support in pursuing my study is invaluable to me.

My parents; I don't think I can find proper words to express my gratitude towards them. They support me from the very beginning of my life that made it possible for me to reach this stage.

I cannot thank enough to my friends who have been with me for a very long time. First and foremost, I express gratitude to my beloved ones; Deniz Atila, Sibel Ataol, Dr. Özge Erdemli (again!), Aylin Acun, Bilgi Güngör, Esin Alpdundar, Alişan Kayabölen and Dr. Bengi Yılmaz. Everything is way much better with them. I will never forget the friendship of Hazal Aydoğdu and Derya Gökçay (Institute Angels) and their contributions to my thesis. I feel very lucky knowing you and thanks for everything. I have learned so much from my senior labmates Dr. Ömer Aktürk, Dr. Ayşegül Kavas and Mert Baki. I appreciate your support and presence. Last but not the least, I would like to thank Zeynep Barçın, Engin Pazarçeviren, Nil Göl, Aydın Tahmasefibar, Ali Deniz Dalgıç and Reza Moonesirad for giving me the opportunity to work in such a warm and nice lab setting.

## TABLE OF CONTENTS

ABSTRACT .....	v
ÖZ.....	vii
ACKNOWLEDGMENTS.....	x
TABLE OF CONTENTS .....	xii
LIST OF TABLES .....	xv
LIST OF FIGURES.....	xvi
LIST OF ABBREVIATIONS .....	xix
CHAPTERS	
1. INTRODUCTION.....	1
1.1. Bone.....	1
1.1.1. Structure and Composition of Bone .....	1
1.1.2. Bone Formation and Regeneration.....	2
1.2. Tissue Engineering .....	5
1.2.1. Bone Tissue Engineering .....	6
1.2.1.1. Bioceramics.....	8
1.2.1.1.1. Hydroxyapatite (HAp) .....	9
1.2.1.2. Microcarrier Systems for Bone Tissue Engineering.....	10
1.2.1.3. Bioactive Agents Used in Bone Tissue Engineering.....	13
1.2.1.4. Adult Stem Cells as Cell Source for Bone Tissue Engineering.....	16
1.3. Aim of the Study.....	18
2. MATERIALS AND METHODS .....	19
2.1. Materials .....	19

2.1.1. Precursors Used for HAp Synthesis .....	19
2.1.2. Precursors for the Preparation of Porous HAp Microcarriers.....	19
2.1.3. Chemicals and Reagents used in Drug Loading and Release Studies .....	20
2.1.4. Chemicals and Reagents used in Cell Culture Studies .....	20
2.2. Experimental Methods .....	20
2.2.1. Synthesis of HAp Powders .....	20
2.2.2 X-Ray Diffraction (XRD) Analyses .....	24
2.2.3. Preparation and Characterization of Porous HAp Microcarriers.....	24
2.2.3.1. Preparation of Porous HAp Microcarriers .....	24
2.2.3.2. Scanning Electron Microscopy Analyses .....	25
2.2.3.3. Particle Size Determination .....	25
2.2.3.4. XRD Analyses .....	26
2.2.3.5 Fourier Transform Infrared Spectroscopy (FTIR) .....	26
2.2.3.6. Microcomputed Tomography (Micro-CT) Analyses.....	26
2.2.3.7. Simvastatin Loading to HAp Microcarriers .....	27
2.2.3.8. DAT Isolation and Coating of HAp Microcarriers.....	28
2.2.3.9 <i>In Vitro</i> Simvastatin Release From DAT Coated and Uncoated HAp Microcarriers.....	29
2.3.4. <i>In Vitro</i> Cell Culture Studies .....	30
2.3.4.1. Isolation of Human Adipose Derived Stem Cells (hASCs).....	30
2.3.4.2. Cell Attachment and Proliferation Studies .....	31
2.3.4.3. <i>In Vitro</i> Differentiation Studies .....	33
2.3.4.4. Microscopical Examinations .....	34
3. RESULTS AND DISCUSSION .....	35
3.1. Characterization of HAp Powders.....	35

3.1.1. XRD Analyses of HAp Powders.....	35
3.1.2. Scanning Electron Microscopy Analyses .....	38
3.2. Optimization of HAp Based Microcarrier Preparation.....	40
3.3. Simvastatin Loading and Encapsulation Efficiency .....	50
3.4. <i>In Vitro</i> Release Profiles of SIM Loaded Microcarriers.....	53
3.5. <i>In Vitro</i> Cell Culture Studies .....	54
3.5.1. Proliferation of Cells on HAp Based Microcarriers .....	54
3.5.2. SEM Analyses of Cell Seeded HAp Based Microcarriers.....	58
3.5.3. Laser Confocal Microscopy of Cell Seeded HAp based Microcarriers....	60
3.5.4. Osteoblastic Differentiation of Saos-2 cells Seeded on HAp Based Microcarriers.....	62
4. CONCLUSIONS.....	67
REFERENCES.....	69
APPENDICES	
A. HPLC CALIBRATION CURVE .....	83
B. ETHICAL APPROVAL.....	85

## LIST OF TABLES

### TABLES

<b>Table 1.</b> Effects of Growth Factors in Bone Regeneration. ....	4
<b>Table 2.</b> Commercially available microcarriers and their properties. ....	12
<b>Table 3.</b> Molar Extinction Coefficients of PrestoBlue™ Reagent. ....	32
<b>Table 4.</b> Experimental Groups and Their Abbreviations.....	33
<b>Table 5.</b> SIM loading and encapsulation efficiencies of HA microcarriers (n=4) ....	53

## LIST OF FIGURES

### FIGURES

- Figure 1.** Molecule structure of Simvastatin. .... 16
- Figure 2.** Flow chart of synthesis of HAp powders by the Sol-Gel method. .... 22
- Figure 3.** Flow chart of synthesis of HAp powders by the co-precipitation method. 23
- Figure 4.** Schematic representation of DAT powder isolation: (A) Human adipose tissue were collected from human donor, (B) lipoaspirate were washed PBS to remove blood cells and oil content(C) washed lipoaspirates was enzymatically digested..... 29
- Figure 5.** XRD patterns of calcined and as synthesized (amorphous) HAp powders prepared by (a) co-precipitation and (b) sol-gel methods. Joint committee on Powders Diffraction Standard (JCPDS) data for HAp crystals are shown for comparison. .... 37
- Figure 6.** XRD patterns of Nano-HAp and sintered Nano-HAp based microcarriers. .... 38
- Figure 7.** SEM images of amorphous HAp powders synthesized by (a) sol-gel and (b) co-precipitation methods. .... 39
- Figure 8.** SEM images of microcarriers prepared with co-precipitated HAp and different surfactants: (a) SDS, (b) Tween 20, and (c) surfactant free. .... 42
- Figure 9.** SEM images of microcarriers prepared with different sized HAp powders (a) commercial Nano-HAp based (<200 nm), (b) synthesized by sol-gel method and (c) synthesized by co-precipitation method. .... 44
- Figure 10.** SEM images sintered microcarriers prepared with (a) 0.5% (b) 0.4% (c) 0.35% and (d) 0.3% Duramax D-3005 dispersant. .... 46

<b>Figure 11.</b> Nano-HAp based microcarriers prepared with water in oil (w/o) emulsion method using 0.3% D-3005 as dispersant. ....	47
<b>Figure 12.</b> Particle size distribution histograms of Nano-HAp based microcarriers prepared by w/o emulsion method. ....	47
<b>Figure 13.</b> 3D images of (a) Microcarriers in Eppendorf after Micro-CT scanning and (b) cross-sectional scanning of single microcarrier. ....	48
<b>Figure 14.</b> SEM images of DAT coated microcarriers at (a) 4 °C and (b) 37 °C. ....	50
<b>Figure 15.</b> FTIR spectra of pure SIM and SIM free and SIM loaded HAp microcarriers in 4000-2000 cm <sup>-1</sup> range. Arrows at wavenumbers 2955 and 2872 cm <sup>-1</sup> are assigned to C-H stretchings of SIM. ....	52
<b>Figure 16.</b> FTIR spectra of pure SIM, SIM free and SIM loaded HAp microcarriers in 2000-400 cm <sup>-1</sup> range. Dashed boxes show the mean (PO <sub>4</sub> ) <sup>3-</sup> bands. ....	52
<b>Figure 17.</b> Cell proliferation of Saos-2 cells on microcarriers. The groups were: HAp microcarriers (HAp), DAT Coated HAp microcarriers (DAT-HAp), HAp microcarriers loaded with 0.01 mg/ml SIM (HAp-0.01), DAT coated HAp microcarriers loaded with 0.01 mg/ml SIM (DAT-HAp-0.01), HAp microcarriers loaded with 0.1 mg/ml SIM (HAp-0.1), DAT coated HAp microcarriers loaded with 0.1 mg/ml SIM (DAT-HAp-0.1), HAp microcarriers loaded with 0.5 mg/ml SIM (HAp-0.5), DAT coated HAp microcarriers loaded with 0.5 mg/ml SIM (DAT-HAp-0.5). ....	56
<b>Figure 18.</b> Proliferation of ASCs on HAp based microcarriers in growth media. Experimental groups were hydroxyapatite (HAp), DAT coated HAp microcarriers (DAT-HAp), HAp microcarriers loaded with 0.01 mg/ml SIM (HAp-0.01), DAT coated HAp microcarriers loaded with 0.01 mg/ml SIM (DAT-HAp-0.01), HAp microcarriers loaded with 0.1 mg/ml SIM (HAp-0.1), DAT coated HAp microcarriers loaded with 0.1 mg/ml SIM (DAT-HAp-0.1), HAp microcarriers loaded with 0.5 mg/ml SIM (HAp-0.5), DAT coated HAp microcarriers loaded with 0.5 mg/ml SIM (DAT-HAp-0.5). ....	57

**Figure 19.** SEM images of Saos-2 cell seeded microcarriers after 24 hours of incubation Cells are shown by arrows..... 58

**Figure 20.** SEM images of ASCs seeded on (a) DAT-HAp-0.5 (b) DAT-HAp-0.1 (c) DAT-HAp-0.01 (d) DAT-HAp (e) HAp-0.5 (f) HAp-0.1 (g) HAp-0.01 (h) HAp after 1 day of incubation. Abbreviations used are HAp microcarriers (HAp), DAT Coated HAp microcarriers (DAT-HAp), HAp microcarriers loaded with 0.01 mg/ml SIM (HAp-0.01), DAT coated HAp microcarriers loaded with 0.01 mg/ml SIM (DAT-HAp-0.01), HAp microcarriers loaded with 0.1 mg/ml SIM (HAp-0.1), DAT coated HAp microcarriers loaded with 0.1 mg/ml SIM (DAT-HAp-0.1), HAp microcarriers loaded with 0.5 mg/ml SIM (HAp-0.5), DAT coated HAp microcarriers loaded with 0.5 mg/ml SIM (DAT-HAp-0.5). ..... 59

**Figure 21.** Z-stack images of cells attached on microcarriers after 24 hours of incubation..... 60

**Figure 22.** Z-stack images of microcarriers that were (a) non-specifically stained with FITC, (b) nuclei of Saos-2 cells stained with PI and (c) cells (stained with PI-red) attached on the microcarriers (stained with FITC–green). ..... 61

**Figure 23.** SEM images and EDX-SEM analysis results of Saos-2 seeded on (a) DAT-HAp-0.5 (b) DAT-HAp-0.1 (c) DAT-HAp-0.01 (d) DAT-HAp after 7 days of incubation in osteogenic media. Spotted areas for EDX analysis were shown by arrows. .... 64

**Figure 24.** SEM images and EDX-SEM spot analysis of Saos-2 seeded on (a) HAp-0.5 (b) HAp-0.1 (c) HAp-0.01 (d) HAp after 7<sup>th</sup> day of incubation in osteogenic induction media. Spotted areas for EDX analysis were shown by arrows..... 65

## LIST OF ABBREVIATIONS

ALP	Alkaline Phosphatase
BCA	Bicinchoninic Acid
BMMSCs	Bone Marrow Derived Stem Cells
BMP	Bone Morphogenetic Proteins
BSA	Bovine Serum Albumin
BTE	Bone Tissue Engineering
CLSM	Confocal Laser Scanning Microscopy
DAT	Decellularized Adipose Tissue
dH <sub>2</sub> O	Distilled Water
ECM	Extracellular matrix
FESEM	Field Emission Scanning Electron Microscopy
FGF	Fibroblast Growth Factor
FITC	Fluorescent Phalloidin
FTIR	Fourier Transform Infrared Spectroscopy
hASCs	Human adipose Tissue Derived Stem Cell
HAp	Hydroxyapatite
HMG-CoA	3-Hydroxy-3-methylglutaryl-coenzyme A

HPLC	High Pressure Liquid Chromatography
IL-1	Interleukin-1
IL-6	Interleukin-6
IGF	Insulin-Like Growth Factor
Micro-CT	Micro-Computed Tomography
MSCs	Mesenchymal Stem Cells
PBS	Phosphate Buffer Saline
PCL	Polycaprolactone
PDGF	Platelet Derived Growth Factor
PET	Polyethyle Terephthalate
PI	Propidium Iodide
PRP	Platelet Rich Plasma
PTFE	Polytetrafluoroethylene
PTH	Parathyroid Hormone
PVA	Polyvinyl Alcohol
PVB	Polyvinyl Butyrate
SDS	Sodium Dodecyl Sulfate
SIM	Simvastatin
TCP	Tri-Calcium Phosphate
TE	Tissue Engineering

TGF- $\alpha,\beta$

Transforming Growth Factor- $\alpha,\beta$

TNF- $\alpha$

Tumor Necrosis Factor- $\alpha$

XRD

X-Ray Diffraction



## CHAPTER 1

### INTRODUCTION

#### 1.1. Bone

##### 1.1.1. Structure and Composition of Bone

Bone is a natural connective tissue that gives internal support to vertebrate body. Besides providing physical support, bone also plays important roles in protecting vital internal organs, controlling mineral balance of the body and leading to movement (Salgado et al., 2004). Bone is a calcified tissue in which bone cells are embedded such as osteocytes, osteoblasts and osteoclasts (Pritchard, 1972). This composite structure of bone consists of organic and inorganic phases. In human body, this composition consists of 30% organic and 70% inorganic. Collagen fibers (mainly collagen Type I) are the main elements of the organic phase and the remaining part contains non-collagenous proteins including osteocalcin, sialoprotein, phosphoproteins, growth factors and blood proteins (Arnett, 2003; Fisher et al., 2007; Van et al., 2008). The inorganic phase is mainly composed of carbonated apatite  $\text{Ca}_9(\text{HPO}_4)(\text{PO}_4)_5(\text{OH})$ . It also includes small amounts of magnesium ( $\text{Mg}^{2+}$ ), carbonate ( $\text{CO}_3^{2-}$ ) and acid phosphate in mineral structure (Clarke, 2008). Biological apatites show different characteristics from synthetic carbonated hydroxyapatite (HAp) nanocrystals like variations in their composition, nanometric crystal sizes, presence of carbonate groups and structure disorders (Salinas et al., 2013).

### 1.1.2. Bone Formation and Regeneration

Bone is a dynamic and active tissue that is able to repair itself to a certain extent which results in production of healthy bone. In healthy adult skeleton, bone tissue maintains its strength and mineral homeostasis through remodeling process. Basically, bone remodeling is the action of bone cell populations in order to replace the existing bone with new bone for preserving the integrity of skeleton (Eriksen, 2010). Two main cell types of bone cells are responsible for bone remodeling: osteoblasts (synthesize and secrete collagen type I and most of the bone proteins) and osteoclasts (mediate bone resorption) (Crockett et al., 2011). The remodeling is initiated by removal of the dead cells from the fracture area by osteoclasts. This stage is called the inflammatory phase. Following stages are local hypoxia and hematoma formation. Hematoma provides surface for cell attachment and proliferation (Damaraju et al., 2014). The formation of hematoma is related to inflammatory response. Production of cytokines including tumor necrosis factor- $\alpha$  (TNF- $\alpha$ ), interleukin-1 (IL-1), and interleukin-6 (IL-6) from aggregated platelets is the first step of the inflammatory response. While IL-6 affects parathyroid hormone (PTH) reaction of bone and regulates differentiation of osteoclasts from hematopoietic precursors, IL-1 induces bone resorption and enhances the effect of IL-6 (Groeneveld et al., 2000). The aggregated platelets have chemotactic activity towards lymphocytes, monocytes-macrophages and fibroblasts (inflammatory cells), and also endothelial cells (Kolar et al., 2011; Salinas et al., 2013). Macrophages are also responsible for the production and secretion of cytokines and various growth factors, which are platelet derived growth factor (PDGF), fibroblast growth factors (FGF), insulin-like growth factors (IGF), the transforming growth factor- $\beta$  (including bone morphogenetic proteins (BMPs) and vascular endothelial growth factor (VEGF) (Hu et al., 2011). The effects of the growth factors in regeneration are summarized in **Table 1**. Repair phase is followed by initial stabilization with cartilage formation. The cartilage is replaced with new bone, and remodeling takes place subsequently. Fracture healing process depends on the oxygen demand of the injured area and

stability of fracture. This process either fails or takes a long time to be completed. It should also be emphasized that bone repair process may be inhibited as a result of an infection, defect size or other causes (Fisher et al., 2007; Hu et al., 2011; Van et al., 2008).

**Table 1.** Effects of Growth Factors in Bone Regeneration.

<b>Bone Morphogenic Proteins (BMPs)</b>	Play an important role in bone generation and regeneration. Stimulate differentiation of Osteoblasts.	(Cheifetz et al., 1996; Chen et al., 2001; Reddi, 2001; Wada et al., 1998; Wozney et al., 1998; Yeh, et al., 2013)
<b>Platelet Derived Growth Factors (PDGF)</b>	Increase wound repair, enhance angiogenesis and cell proliferation in cultures of osteoblast-like cells isolated from adult bone.	(Fisher et al., 2007; Kakudo et al., 2008)
<b>Fibroblast Growth Factor (FGF)</b>	Regulates mitogenesis, differentiation, protease production, receptor modulation and cell maintenance.	(Fisher et al., 2007; Jeong et al., 2010)
<b>Vascular Endothelial Growth Factors (VEGF)</b>	Induces angiogenesis and bone formation from osteoprogenitor cells, as well as extracellular matrix synthesis.	(Fisher et al., 2007; Goad et al., 1996; Kolar et al., 2011)
<b>Transforming Growth Factors (TGFs)</b>	Trigger differentiation, growth and extracellular matrix synthesis.	(Fisher et al., 2007; Nikolidakis et al., 2008)
<b>Insulin-like Growth Factor (IGF)</b>	Improves osteoblast activity, production of type I collagen and VEGF expression from osteoblasts. Decreases collagen degradation, inhibits apoptosis and regulates growth in various cell types.	(Goad et al., 1996; Meinel et al., 2001; G. R. Mundy, 2000)

Bone formation process is monitored by several techniques including bone markers such as alkaline phosphatase (ALP), collagen type I, osteopontin, osteocalcin and bone sialoprotein. ALP and type I collagen serve as early marker while bone sialoprotein and osteocalcin are considered as late marker (Fisher et al., 2007).

## **1.2. Tissue Engineering**

Today, millions of people suffer from failure of organs and shortage of organ donations. Current treatments are based on the use of commercial inert biomaterials, autografts or allografts (Buchanan et al., 1990; Joon et al., 2007). Autografts are good sources; however, they have many disadvantages such as the limited mass of autografted organ and the risk of generation of complications. The use of allografts bears risks including disease transmission and immune response. Alternatively, metals, polymers and composites are used as biomaterials in preclinical and clinical studies (Bohner et al., 2013; Vats et al., 2003). Usually, metals such as stainless steel and titanium are used for permanent fixation of bone. However, corrosion susceptibility of metal implants and infection of surrounding tissue limit their uses in host tissue (Albrektsson et al., 2001). Moreover, mechanical properties of metals are greater than natural bone tissue, therefore; it leads to resorption of surrounding tissue causing removal of whole implant (Mistry et al., 2005). Synthetic and natural polymers are preferred for scaffold preparation for tissue regeneration because of their resemblance to natural tissues, ease of production and control over physical structure according to the needs. However; each type of material has some drawbacks, and none of them can accomplish autografts functionality completely in current clinical studies (Fisher et al., 2007; Salgado et al., 2004; Van et al., 2008).

In order to achieve complete recovery of the original tissue, tissue engineering is an alternative approach. Tissue repair/regeneration process requires some important parameters that need to be provided including appropriate cell types, growth factor-enhanced biocompatible scaffolds that provide intercellular communications and

cell-matrix interactions (Nerem, 2007; Salgado et al., 2004). One of the differences between tissue grafts and biomaterials is that; tissue graft contains living cells and tissue-inducing substances. At this point, as already discussed, tissue engineering concept includes all of the graft materials features except its drawbacks. Research studies are currently in progress to develop cell-containing scaffolds to create replacement tissues that remain interactive with host tissue after transplantation (Van et al., 2008).

### **1.2.1. Bone Tissue Engineering**

There are many people in the world suffering from skeletal defects that require bone-graft procedures. Due to aging of the populations, these demands will increase. As it is already discussed above in general manner, tissue engineering is a promising approach for bone tissue repair as an alternative to conventional therapies. There are two important concepts to achieve bone regeneration by using scaffold guided tissue engineering: osteoconductivity and osteoinductivity. The osteoconductivity is the ability of the scaffold to provide surface for cell attachment and growth. Osteoconductive materials permit bone growth into interconnected pore channels. On the other hand, osteoinductivity is a specialty of the material that stimulates undifferentiated and pluripotent cells to differentiate into bone forming cell lineages (Albrektsson and Johansson, 2001; Dimitriou et al., 2011). In addition to being osteoconductive and osteoinductive, tissue engineered scaffolds must provide several important properties to achieve optimal bone healing. Scaffolds must be biodegradable and the degradation rate of the material must match the rate of tissue regeneration. Furthermore, the scaffolds must provide interconnected pore channels to enhance tissue ingrowth, vascularization and nutrient transport for the internally localized cells. There are several factors that affect the scaffold fabrication and accessibility, such as cost effectiveness, shelf- life period and manufacturability.

Investigated biomaterials for bone tissue engineering include non-resorbable materials (i.e., polytetrafluoroethylene (PTFE), polyethylene terephthalate (PET)) (Vats et al., 2003), biodegradable natural and synthetic polymers (i.e., collagen, polylactides (PLLA, PDLA), polycaprolactone (PCL)) (Gray et al., 1998), bioactive ceramics (HAp, Bioglasses) and composites (i.e., generally combination of bioactive ceramics with polymers such as PCL-HAp composite material) (Rizzi et al., 2001; Tanner, 2010).

Non-resorbable materials are generally used in periodontal inserts and sutures (Vats et al., 2003). PTFE is mostly used as a non-resorbable scaffold for bone regeneration. It has been shown that PTFE enhanced bone healing in animal models (Dupoirieux et al., 2001; Kellomäki et al., 2000). Besides being non-resorbable materials, biodegradable polymers are more preferable for engineering of bone. Especially, natural polymers have been widely used in tissue engineering applications owing to their low toxicity and lower possibility of immune rejection than other material types. However, their low mechanical strength and complex structure limit their uses. Therefore, improving mechanical strength of natural polymers by using different chemicals (i.e., crosslinkers) is needed and this strategy also has some drawbacks (Vats et al., 2003). Synthetic polymers are promising to remedy these problems. Their structure can be tailored to adjust mechanical properties. However, byproducts like monomers and catalysts that have used in the synthesis of such polymers may cause cytotoxic effect in implanted area (Fisher et al., 2007).

One of the appropriate materials for bone tissue is bioceramics. Bioceramics is a subcategory of ceramics, which include oxides, phosphates, carbonates, nitrides, carbides, and glasses which closely mimic mineral phase of natural bone. These compounds are known for strong binding ability with bone tissue (Pattanayak et al., 2010). HAp is a well-known bioceramic that has showed excellent compatibility with surrounding tissue (Wei and Ma, 2004).

Composites, combination of two or more different types, are mostly used in bone tissue regeneration. They show unique properties that are quite different from the individual materials that make up the composite structure. Therefore, it is more feasible to adjust desired stiffness and mechanical properties of composites by varying the composition and morphology of the constituents (Kellomäki et al., 2000). In bone tissue engineering applications, scaffolds usually contain bioceramics as inorganic compounds to enhance the osteoconductivity and polymers as the organic part to increase stiffness and flexibility (Johari et al., 2012; Kellomäki et al., 2000).

#### **1.2.1.1. Bioceramics**

In materials science, ceramics are defined as inorganic materials with polycrystalline structures. Ceramics, formed by metal and nonmetal elements, include metallic oxides such as aluminum oxide  $\text{Al}_2\text{O}_3$ , silicates, carbides, sulfides, and selenides (Joon Park, 2008). Ceramics used in clinical applications are called bioceramics (Pattanayak et al., 2010). These types of ceramics are widely used in applications of bone tissue replacement. Bioceramics and their composites with polymers or metals have been used in the bone tissue engineering including polycrystalline ceramics (HAp), glass, glass-ceramics (A-W glass ceramics) or as composites like polycaprolactone (PCL)-HAp. For example, titanium with bioceramic coating and alumina are used in clinical applications for bone tissue replacement because of their load bearing characteristics (Joon Park, 2008). Ceramics can exhibit different characteristics in body. Bioinert ceramics are nontoxic and biologically inactive. When those types of ceramics are implanted in defect site, the material is covered by a fibrous tissue of variable thickness. Although bioinert materials are good for replacement applications, they are not suitable materials for providing bone regeneration. There is another type of ceramics that can provide bone tissue regeneration. Those are calcium phosphate ceramics. Calcium phosphates are bioactive ceramics that are non-toxic and biologically active (osteoconductive) (Champion, 2013). Once they are implanted, they form interfacial bonding with

surrounding tissues. Generally, tri-calcium phosphate and HAp are preferred for regenerative purposes (Rojbani et al., 2011; Zheng et al., 2011). These ceramics have a brittle polycrystalline structure. Their mechanical properties differ depending on the particle size, the amount of grain boundaries and porosity (Salinas et al., 2013).

In natural environments, bioceramics can be degraded by (i) solution-mediated, (ii) cell-mediated mechanisms or (iii) both of the mechanisms. Solution-mediated mechanism is a physiochemical degradation. Under physiological environment, their degradation is promoted which eventually causes deterioration of mechanical properties. Calcium phosphate ceramics undergo dissolution-precipitation cycle in natural aqueous environment before dissolving (Van et al., 2008). In body, cellular degradation is performed by osteoclasts (Eriksen, 2010).

#### **1.2.1.1.1. Hydroxyapatite (HAp)**

HAp is the main component of hard tissue such as bone, dentin and enamel. Hydroxyapatite [ $\text{Ca}_{10}(\text{PO}_4)_6(\text{OH})_2$ ] is one of the calcium phosphate ceramics widely used in bone regeneration applications because of its similarity to inorganic component of bone (Ravaglio and Krajewski, 1992). Bone tissue has biologic hydroxyapatite that has ratio of Ca/P < 1.67 (Valletregi, 2004). HAp ceramics may be derived from either natural sources or synthetically. Since it is bioactive, biocompatible and osteoconductive, HAp can support and provide structural framework for surrounding during the host bone regeneration. HAp has been widely used in clinical applications such as bone defects, middle ear prostheses, and craniofacial repair. Moreover, it has been mentioned that HAp based scaffold systems also have great potential in delivery of drugs and biomolecules (M.-H. Hong et al., 2011; Santoni et al., 2007). Recent studies showed that nano sized HAp crystals with appropriate stoichiometry, size (<100 nm) and purity have great potential to induce bioactivity to the scaffold (Sadat-Shojai et al., 2013; Valletregi, 2004). Additionally, in biological environment, calcium ( $\text{Ca}^{+2}$ ) release from the nano

sized HAp based scaffolds is similar to the release observed from natural bone minerals (L. Wang and Nancollas, 2009). It has been reported that when the size of HAp crystals is decreased from micron to nano scale, surface reactivity was enhanced resulting in higher host tissue and scaffold interaction (Cai et al., 2007; Dorozhkin, 2010). It was also emphasized that the use of nano sized HAp decreases apoptic cell death (Dorozhkin, 2010; Li et al., 2008). Because of the surface roughness of nano powders, cell adhesion, proliferation, differentiation and osteointegration were improved in *in vitro* studies (Dorozhkin, 2010; Y. Wang et al., 2010; Webster, 2001). These properties of HAp shorten the regeneration period of the implanted tissue (Murugan and Ramakrishna, 2005; Sadat-Shojai et al., 2013; Van et al., 2008).

#### **1.2.1.2. Microcarrier Systems for Bone Tissue Engineering**

Microcarrier technology has become vital practically and commercially for production of biological products such as vaccines, antibodies, enzymes and hormones. In recent years, the microcarriers have often been used for cell culture studies in tissue engineering applications. These cell culture studies are termed suspension culture and provide some important advantages. These are:

- (i) Spherical particles provide large surface to volume ratio, therefore the microcarriers improve cell attachment, migration and proliferation in *in vitro* culture systems (Barrias et al., 2005),
- (ii) Suspension culture requires less cell density and cell culture ingredients than monolayer cell culture. When compared to monolayer culture, the yield is increased 100-fold by utilizing microcarriers. The application of microcarriers has involved expansion of stem cells in many studies (Goh et al., 2013; Kehoe et al., 2010),

- (iii) Microcarrier culture requires a more simplified preparation procedure compared to the other types. Medium can be easily removed from cells and a decrease in the risk of contamination was reported to decrease (Ma and Zhi-Guo, 2013; Park and Pe, 2013).

Spherical microcarriers are commonly used in tissue engineering applications. The microcarriers are made of wide range of materials including synthetic and natural polymers, bioceramics and composites. There are commercially available microcarriers in the market (**Table 2**).

It has been reported that microcarriers made from wide range of materials were shown to have great potential for bone tissue regeneration (Barrias et al., 2005). To achieve similarity with the microstructure of bone matrix, porous microcarriers are generally preferred, as cells can penetrate and attach each other at the inner sides of pores and vascularization can be induced in pore channels (Hong et al., 2009). In addition to other advantages, interconnected porous ceramic microcarriers preserve their mechanical strength even after heat treatment at high temperatures (Silva et al., 2007). For preparation of these solid-state spherical particles, either emulsion or spray drying method is used. In these methods, bioceramic powders are generally mixed with a binder such as polyvinyl alcohol (PVA) (Yang et al., 2011), polyvinyl butyral (PVB) (S-J Hong et al., 2009) and gelatin (Teng and Chen, 2007). Binded powders are then subjected to high temperature heat treatments for crystallization (Oliveira and Mano, 2011; Jeong-hui Park, 2013).

Previous studies propose different strategies for tissue regeneration. Most of them include the use of growth factors or inductive agents that may promote tissue regeneration (Oliveira and Mano, 2011). Polymeric, composite or ceramic based microcarriers have been used to deliver these therapeutic factors to the implantation area (Chou et al., 2013; Lin et al., 2010). Loading of bioactive agent to these delivery systems is achieved by diffusion or with use of specific interactions between agents and carrier components (Oliveira and Mano, 2011).

**Table 2.** Commercially available microcarriers and their properties.

Company /Product Name	Particle Size (µm)	Materials	Properties	Target Cell Type	References
Pall/ Solohill® microcarrier beads Collagen coated	125-212	Polystyrene Beads	Designed to support cell growth at a variety of scales: spinner flasks, micro bioreactors, small to large scale stirred tank bioreactors, rocking platforms and microgravity bioreactors.	Adherent diploid cells	Malda et al., 2003
GE Healthcare /Cytopore 2	200-280	Cellulose	Principally designed for use in suspension culture systems.	Anchorage- dependent cells (require a higher charge capacity for optimal cell growth)	Y. Yang et al., 2007
Sigma/ Cultispher®- S standard porosity, High thermal stability	130-380	Gelatin	Used for increasing surface area for growth of cells <i>in vitro</i> capabilities. An additional advantage of the product is that the matrix can be dissolved with proteolytic enzymes ensuring harvest of cells with almost 100% viability.	Anchorage- dependent cells (require a higher charge capacity for optimal cell growth)	Malafaya et al., 2007

### **1.2.1.3. Bioactive Agents Used in Bone Tissue Engineering**

In tissue engineering approach, an ideal scaffold should provide suitable environments to the cells *in vitro* and *in vivo* cultures (Hoshiya et al., 2010). Besides scaffolds and tissue specific cells, bioactive agents are also important for cell proliferation and differentiation in defect site. In bone tissue engineering (BTE), bioactive agents which are also called as osteoinductive agents have been used in bone regeneration. These include growth factors such as BMPs, VEGF, FGF, PDGFs and also statins (Tezcaner and Keskin, 2011). TGF- $\beta$ , BMPs, PDGF and VEGF are also widely used bioactive agents in BTE (Dimitriou et al., 2005). In clinical studies, BMP-2 has been found as the most effective growth factor for regeneration of bone tissue (Groeneveld and Burger, 2000). It has been reported that BMP-2 containing scaffolds induce bone tissue growth and integration in the defect site (Partridge et al., 2002). There are many studies in which bioactive agent loaded carriers were used for *in vivo* and *in vitro* bone regeneration studies (Lieberman et al., 2002; Okuda et al., 2003). The bioactive agents that have been used to induce new tissue formation are either isolated or purchased commercially. Natural extracellular matrix (ECM) is responsible from regulation of signal transduction activated by various bioactive agents such as growth factors and cytokines. Structural, chemical and mechanical properties of ECM molecules vary in different tissues and organs. ECMs have complex structures composed of different types of proteins, proteoglycans growth factors and cytokines. It is difficult to achieve mimicking the whole natural tissue through using synthetic ECMs. This led researchers to use decellularized natural tissue matrix as constructs for tissue regeneration. Through this method, scaffolds can have tissue specific ECMs including proteins and remaining tissue and cell specific micro and nano environment (Hoshiya et al., 2010). In previous clinical studies, biological scaffolds composed of decellularized-ECM of tissues or organs have been successfully applied on patients. Such scaffolds have been used in skin (Mason, 2005), urinary bladder (Badylak et al., 2011), trachea (Zang et al., 2012) and

heart valve replacements and regenerations (Hopkins et al., 2013, Cheng et al., 2014).

In bone tissue engineering, decellularized bone (DBM) and cartilage matrix are the most common constructs used. Among those, decellularized bone tissue has shown great potential. In literature, several *in vitro* studies have shown that DBM has the potential to stimulate osteogenesis in human adipose-derived (Shi et al., 2012) and bone marrow derived mesenchymal stem cells (B.-W. Park et al., 2012). Furthermore, there are clinical studies in which DBM has been used as a tissue construct in reconstruction of osteochondral defects (Upton and Glowacki, 1992). Unlike autografts and allografts, the use of decellularized constructs reduce operation time, donor site morbidity and lack of donor tissue problems (Cheng et al., 2014).

Decellularized adipose tissue (DAT) is among the most widely used tissue construct for tissue engineering applications. DAT provides a well-preserved 3D structured extracellular matrix. Such structures may contain fibrous collagen network including type I, III, V and VI (Flynn et al., 2006). Moreover, DAT also has other extracellular matrix components, such as proteoglycan, glycoprotein, glycosaminoglycan, elastin fibers, fibronectin and laminin (Turner et al., 2012). Similar to bone tissue, it has fibronectin, glycoprotein and proteoglycans (Benders et al., 2013; Cheng et al., 2014). In extracellular matrix of bone, fibronectin contributes osteogenic differentiation and wound healing (Cheng et al., 2014) and proteoglycans are the reservoirs of several growth factors and glycoproteins that interact with collagen fibrils to provide mechanical stability to ECMs (Benders et al., 2013). The most important feature of the DAT structure for engineering bone is that it has collagen type I proteins (Turner et al., 2012). According to Gibson et al., DAT has great potential for osteogenic differentiation of human adipose tissue derived stem cells (ASCs) (Gibson et al., 2014). They tried to produce composite electrospun Poly- $\epsilon$ -caprolactone (PCL) nano fibers with 10% DAT. According to their results, there are factors in fat tissue that promote osteogenetic activity such as BMPs, laminin and

fibronectin. Alternatively, these decellularized matrices may induce immune response that triggers differentiation of ASCs (Gibson et al., 2014).

In addition to decellularized matrices, platelet rich plasma (PRP) derived from blood have been also widely used as natural bioactive agent resource. PRP is a concentrate of platelets in a small volume of blood plasma. Platelets are capable of inducing stem cells to differentiate into both osteogenic and angiogenic cells (Cinotti et al., 2013).

Statins are cholesterol lowering drugs. They inhibit 3-hydroxy-3-methylglutaryl coenzyme A (HMG-CoA) reductase in the mevalonate pathway (Song et al., 2003). Moreover, their inhibitory effects on tumor growth and metastasis, and promotion of angiogenesis, and t-lymphocyte suppression have been reported in recent studies (Y. Zhang et al., 2014). It was shown that bone healing have been enhanced when sufficient doses of statins which are used for lowering human cholesterol level were applied to rodents (Mundy, 1999). Statins have different molecular structures such as fluvastatin, simvastatin and mevastatin (Mundy, 1999). Simvastatin (SIM) is one of the statins (**Figure 1**) that has remarkable osteoinductive effect (Song et al., 2003). It was reported that SIM induces mRNA expression and synthesis of BMP-2 in bone healing and regeneration process. It was also indicated that SIM increased mineral density of bone in postmenopausal women with high blood cholesterol (Lupattelli et al., 2004). In recent studies, 1  $\mu$ M of SIM have been found effective for bone healing with *in vivo* applications in rodent animal models (Zhou et al., 2010). According to Stein et al., local application of SIM is more effective than oral administration (Stein et al., 2006). Compared to systemic application, local delivery of SIM requires fewer amounts for osteogenesis because if it is delivered in systemically most of SIM metabolized in liver (Zhao et al., 2014). According to Gutierrez et al., topically applied or continuously released statins were 50 to 80 times more effective than systemically applied statins in *in vivo* studies (Gutierrez et al., 2008).

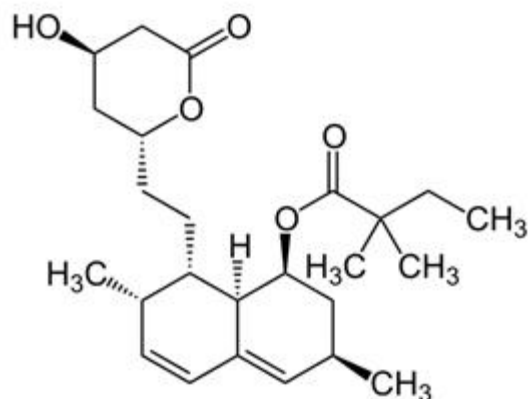


**Figure 1.** Molecule structure of Simvastatin.

#### **1.2.1.4. Adult Stem Cells as Cell Source for Bone Tissue Engineering**

Tissue engineered constructs have three important components: scaffolds, bioactive agents and cells. Among those, cells are the most important components of the engineered tissue (Bianco and Robey, 2001). Seeding autologous cells onto engineered bone grafts are required for an ideal tissue regeneration process (Damaraju and Duncan, 2014). Regeneration is achieved by the suitable cell type and environment. Stem cells are the most suitable option for tissue engineering due to their ability to differentiate into functional cells of targeted tissue. Stem cells have two important properties; self-renewal and differentiation (Bianco and Robey, 2001). Self-renewability is the ability to make identical copies of the cells, whereas the differentiation allows the cell to transform into other type of cells in the body (Van et al., 2008).

Stem cells can be classified as; embryonic and somatic (adult). In biological systems, embryonic development and growth are carried out by the embryonic stem cells, and adult stem cells are responsible for growth, tissue maintenance, regeneration and repair of damaged tissue (Sottile et al., 2003; Van et al., 2008).

Researches are focused on mesenchymal stem cells (MSCs) due to their therapeutic effect in tissue regeneration. MSCs are multipotent stem cells, meaning that they have the potential to differentiate into multiple, but limited cell types such as osteocytes, chondrocytes and adipocytes. They are found in undifferentiated and they have the ability of self-renewal (Jaiswal et al., 2000; Pittenger, 1999). They can be isolated from bone marrow, umbilical cord blood and adipose tissue (Strem et al., 2005). There are various types multipotent stem cells isolated from different tissue sources, such as adipose derived stem cells; bone marrow derived stem cells (BMMSCs) (Im et al., 2005). BMMSCs are important source of multipotent stem cells (Uter, 2006). They can be isolated from bone marrow however; the procedure is problematic and inefficient with respect to the isolated cell number. Moreover, aging is an important parameter for BMMSCs, since differentiation potential and obtained cell number decrease with aging (Im et al., 2005; Uter, 2006). Instead of BMMSCs, adipose derived mesenchymal stem cells (ASCs) are currently being used (Uter, 2006). In recent years, with increasing number of obesity patients, there are more than 400.000 liposuction surgeries made annually. Thus, scientists have focused on human subcutaneous adipose tissue for isolation of adult and somatic stem cells (Bunnell et al., 2008). It is reported that these cells are also multipotent and they can differentiate into adipose, epithelial, muscular, bone, nerve and heart tissue (Im et al., 2005; Safford et al., 2004; Strem et al., 2005; Zanetti et al., 2013).

In order to differentiate stem cells towards a desired lineage, culture media supplements and promoter environment are necessary (Fisher et al., 2007; Yoshimura et al., 2007). It has been reported that MSCs differentiate into bone tissue in an appropriate microenvironment of a suitable scaffold (Jaiswal et al., 2000). For osteogenic differentiation dexamethasone, ascorbate, and  $\beta$ -glycerophosphate are used in induction medium *in vitro* (Jaiswal et al., 2000; Ogawa et al., 2004). Differentiation of MSCs into bone phenotypes can be determined by *in vitro* assays. When MSCs differentiate into osteogenic lineage, they secrete various bone specific

proteins (alkaline phosphatase, osteonectin, osteopontin, etc) (Fisher et al., 2007; Van et al., 2008).

### **1.3. Aim of the Study**

In recent years, microcarriers have gained importance for clinical applications in order to provide healing critical shaped and sized defect area. Microcarriers can be prepared in spherical form with interconnected pore structure. The aim of the study was to develop DAT coated SIM loaded HAp based microcarrier systems as cell delivery system and to characterize them *in vitro*. Porous HAp microcarriers were prepared with HAp powders in different size range by water in oil emulsion method. The emulsified particles were sintered at 1200°C for removing the organic phase and increasing the stability and elasticity of HAp spherical granules. In this study, SIM was used as osteoinductive agents to induce osteogenic differentiation of cells. After SIM loading to HAp microcarriers, they were coated with human decellularized adipose tissue (DAT) components for maximizing cell adhesion, proliferation and osteoblastic differentiation, as well as for controlling release of SIM from microcarriers. Surface morphology and size of the microcarriers were examined by scanning electron microscopy (SEM) and dynamic light scattering method. Interconnectivity of the pores was studied by Micro-CT analysis. Drug loading studies were performed with both DAT coated and uncoated HAp microcarriers. For biocompatibility and functionality analyses, *in vitro* cell culture tests were performed using adipose derived stem cells (ASCs) and Saos-2 Human osteosarcoma cell line.

## CHAPTER 2

### MATERIALS AND METHODS

#### 2.1. Materials

##### 2.1.1. Precursors Used for HAp Synthesis

The precursors used in HAp synthesis, calcium nitrate tetrahydrate ( $\text{Ca}(\text{NO}_3)_2 \cdot 4\text{H}_2\text{O}$ ) and di-ammonium hydrogen phosphate ( $(\text{NH}_4)_2\text{HPO}_4$ ), were obtained from Merck, Germany. Ammonium hydroxide ( $\text{NH}_4\text{OH}$ ) and nitric acid ( $\text{HNO}_3$ ) that were used for controlling solution pH during synthesis of HAp powders were the products of Sigma (USA).

##### 2.1.2. Precursors for the Preparation of Porous HAp Microcarriers

HAp based microcarriers was prepared by water in oil (w/o) emulsion method. The aqueous component was Type-A gelatin from porcine skin (Sigma, USA) and Mowiol 4-98 with a molecular weight of  $27000 \text{ g mol}^{-1}$  (Aldrich, Germany). As a porogen, camphene was purchased from Aldrich (USA). Tween-20 (Sigma, USA) and sodium dodecyl sulfate (SDS; Bio-Rad, CA) were used as surfactants. Duramax<sup>®</sup> D-3005, ceramic dispersant, was a gift from DOW Chemical company, Turkey. Triton X-100 was the product of Sigma (USA). Corn oil (Komili, Turkey) was used as the oil component in emulsion systems.

### **2.1.3. Chemicals and Reagents used in Drug Loading and Release Studies**

Inertsil ODS-3 C18 column were purchased from GL Sciences, Japan. Simvastatin (HPLC grade,  $\geq 97\%$ , solid) was obtained from Sigma, Canada. Methanol (Chromasolv<sup>®</sup>, HPLC grade,  $\geq 99.9\%$ ), acetonitrile (Chromasolv<sup>®</sup> Plus, HPLC grade,  $\geq 99.9\%$ ) were the products of Sigma-Aldrich, Israel.

### **2.1.4. Chemicals and Reagents used in Cell Culture Studies**

Human Osteosarcoma cell line, Saos-2 (HTB-85) was purchased from ATCC (USA). Dulbecco's Modified Eagle Medium (DMEM), Fetal Bovine Serum (FBS), Penicillin/ Streptomycin, Tyripsin-EDTA was purchased from Biochrom (Germany). CellStar<sup>®</sup> suspension cell culture plates were the products of Greiner bio-one (USA), Type IA collagenase was obtained from Sigma (USA), Alkaline Phosphatase (ALP) Assay Kit was purchased from Abcam, (USA). Bicinchoninic acid (BCA) reagent was the product of Sigma (Germany). PrestoBlue<sup>®</sup> cell viability Reagent was purchased from Life Technologies, Poland. Fluorescent Phalloidin and propidium iodide were obtained from Invitrogen (USA). Hexamethydisilazane (HMDS), was purchased from Sigma (USA).

## **2.2. Experimental Methods**

### **2.2.1. Synthesis of HAp Powders**

Two different solution-based synthesis approaches were used to synthesize HAp powders. The first method was sol-gel based route where proper amounts (in regard to stoichiometric HAp) of calcium nitrate tetrahydrate ( $\text{Ca}(\text{NO}_3)_2 \cdot 4\text{H}_2\text{O}$ ), phosphoric acid ( $\text{H}_3\text{PO}_4$ ) and ammonia solution were first mixed to obtain a parent solution (Sanosh et. al., 2009). Ammonia was added into phosphoric acid solution to obtain a highly alkaline solution (pH 10) to favor HAp gel precipitation and 1 M calcium

nitrate tetrahydrate solution was added into phosphoric acid-ammonia solution. The mixed solution was then continuously stirred for 1 hour with a magnetic stirrer during which, the pH of the solution was kept constant by the addition of ammonia. After 1 hour stirring, the gel-like solution was aged in ambient atmosphere for 24 hours at  $25\pm 1$  °C. The final gel was dried at 65°C for 24 hours in a drying oven (Nüve, Turkey). In order to remove excess  $\text{NH}_4^+$  and  $\text{NO}_3^-$ , the dried powders were washed several times with  $\text{dH}_2\text{O}$ . After washing, the powders were calcined in an electrical furnace (Protherm, Turkey) at 900 °C for 30 min with a heating rate of 10 °C/min (**Figure 2**).

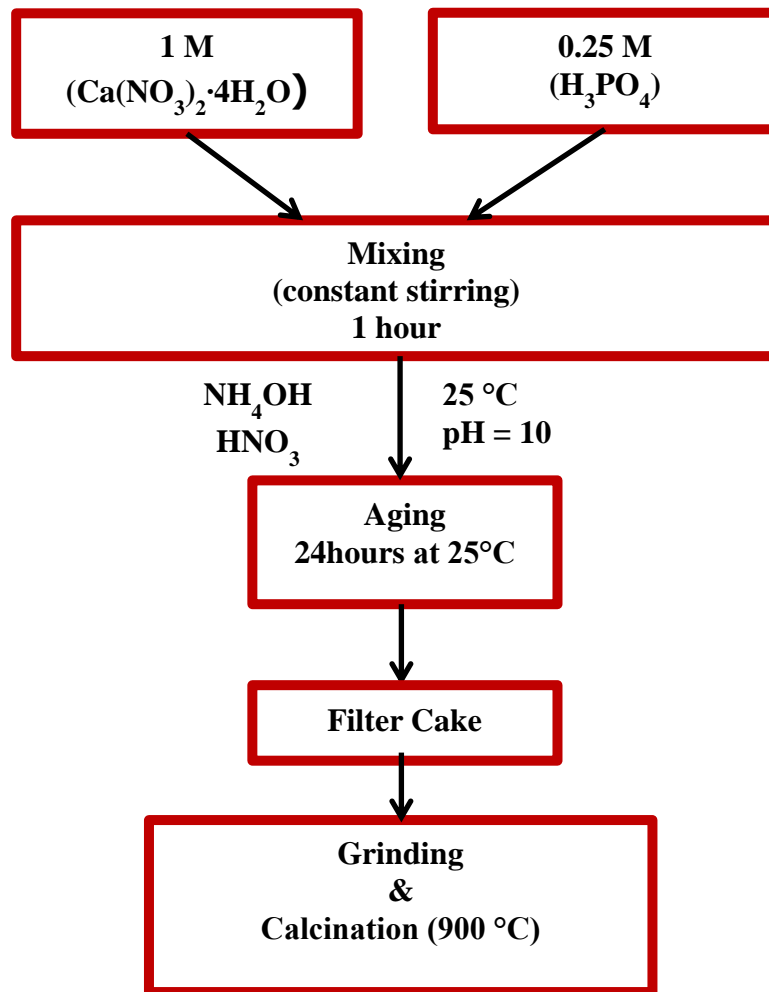


**Figure 2.** Flow chart of synthesis of HAp powders by the Sol-Gel method.

In the second method, HAp powders were synthesized by the co-precipitation method (Simsek, 2002). HAp powders were precipitated directly from an aqueous solution obtained by drop-wise (10 ml/min) addition of 0.1 M  $(\text{NH}_4)_2\text{HPO}_4$  into 0.167 M  $\text{Ca}(\text{NO}_3)_2 \cdot 4\text{H}_2\text{O}$  solution under constant stirring. The solution pH was kept

constant at 10, by the addition of  $\text{NH}_4\text{OH}$  and  $\text{HNO}_3$ . The precipitate solution was further aged at  $\sim 60^\circ\text{C}$  overnight. The precipitates were filtered and washed several times with  $\text{dH}_2\text{O}$  in order to remove nitrate salts. The precipitate solution was ultrasonically treated for 15 min after it was resuspended in  $\text{dH}_2\text{O}$  during each washing step. The solid powder extracts were then washed with 96% ethanol to remove the excess water from the surface of the precipitates and to minimize agglomeration of the fine powders. The filtered precipitate cakes were further dried at  $105^\circ\text{C}$  overnight in ambient air. The dried powders were calcined in an electrical furnace at  $900^\circ\text{C}$  for 30 min with a heating rate of  $10^\circ\text{C}/\text{min}$  (**Figure 3**).

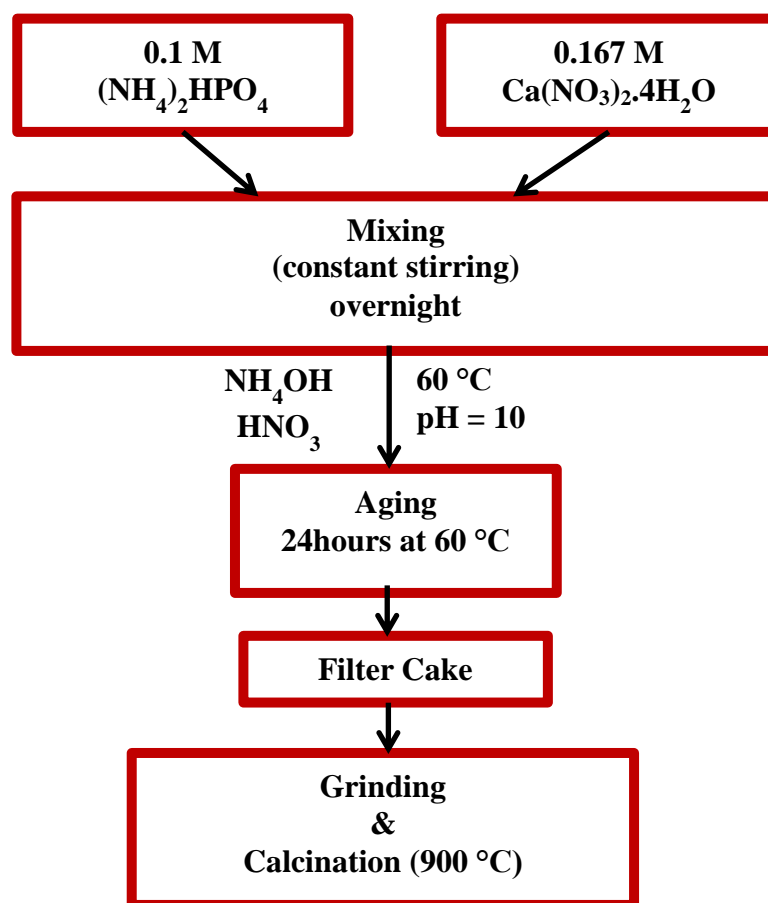


**Figure 3.** Flow chart of synthesis of HAp powders by the co-precipitation method.

## **2.2.2 X-Ray Diffraction (XRD) Analyses**

The phase purity and the crystallinity of the as-precipitated and as-synthesized HAp powders obtained from precipitation and sol-gel routes, respectively, were examined with a Rigaku DMAX 2200 diffractometer, Japan. XRD spectrum of commercial Nano-HAp powder (Sigma, USA) was also acquired for comparison. XRD analyses were performed after calcining the as-synthesized and as-prepared powders in order to reveal the structural evolution of the prepared powders after heat treatment. The diffraction tests were performed for diffraction angle ( $2\theta$ ) range of  $20^\circ$ - $60^\circ$ , at a scanning rate of  $2^\circ/\text{min}$  using Cu-K $\alpha$  radiation and an operation voltage of 40 kV and a current of 30 mA.

## **2.2.3. Preparation and Characterization of Porous HAp Microcarriers**

### **2.2.3.1. Preparation of Porous HAp Microcarriers**

The HAp-based microcarriers were prepared by water in oil (w/o) emulsion method (Yang et al. 2011). In order to elucidate the effect of HAp particle size on microsphere formation HAp powders of different particle sizes were used, namely; (i) commercial Nano-HAp (particle size  $<200$  nm, Sigma, USA), (ii) HAp synthesized by sol-gel method (particle size  $\sim 40$   $\mu\text{m}$ ) and (iii) HAp powders (particle size  $\sim 40$   $\mu\text{m}$ - $70$   $\mu\text{m}$ ) obtained by co-precipitation.

In preparation of microcarriers, camphene was mixed with HAp powders at a HAp to Camphene ratio of 1:0.9 (**wt/wt%**) at  $60^\circ\text{C}$  by using a magnetic stirrer. For each gram of HAp powder, 2 ml 10% porcine skin gelatin in 2% (v/wt%) Mowiol solution was added into camphene-HAp slurry. In order to achieve an optimal particle dispersion, three different surfactants (0.3 wt%) were added into gelation solution, sodium dodecyl sulfate (SDS), Tween-20, and poly-ammonium salt (Duramax<sup>®</sup> D-3005) together with 0.2% Triton X-100. After the addition of gelatin solution, the mixture was then stirred for 30 min and then the whole solution was poured into 250

ml of corn oil and stirred at 480 rpm overnight. The solution was rapidly solidified in an ice cooled bath at 4 °C for 5 min. They were then filtered and rinsed with acetone. Filtered products were stored at -20 °C for 24 hours and camphene was sublimated by a freeze-drier (Labconco, USA). Dried products were first heated to 500 °C with 3°/min and kept at that temperature for 1 hour. The products were further heated to 1200 °C with 5°/min increase and kept at this temperature for 3 hours (S-J Hong et al., 2009; Yang et al., 2011).

### **2.2.3.2. Scanning Electron Microscopy Analyses**

The morphology and microstructural characteristics (agglomeration state and particle size) of calcinated HAp powders were examined by field emission scanning electron microscope (FESEM) (FEI Quanta 400F, USA). The surface morphology and pore structures (size, connectivity) of the sintered HAp based microcarriers were also investigated. The samples were gold sputtered before imaging to minimize the charging problem.

### **2.2.3.3. Particle Size Determination**

In addition to SEM analyses (Section 2.2.3.2), the particle size of the synthesized HAp microcarriers was also determined using laser diffraction particle size analyzer (Malvern, Mastersizer 2000, UK with Hydro 2000S accessory). Microcarriers were ultrasonically dispersed in DI water prior to analyses.

#### **2.2.3.4. XRD Analyses**

The effect of sintering on the structural characteristics of HAp microcarriers was also investigated. HAp microcarriers were crushed into powder form for XRD examination. The diffraction tests were performed for diffraction angle ( $2\theta$ ) range of  $20^\circ$ - $60^\circ$ , at a scanning rate of  $2^\circ/\text{min}$  using Cu-K $\alpha$  radiation and an operation voltage of 40 kV and a current of 30 mA.

#### **2.2.3.5 Fourier Transform Infrared Spectroscopy (FTIR)**

Chemical and phase composition of materials of the HAp microcarriers were studied by FTIR analysis using FTIR spectrometer (Bruker IFS 55, Switzerland). Samples were observed with ATR and pellet technique and the spectra were recorded from 400 to  $4000\text{ cm}^{-1}$ . Additionally, the loading of SIM was also verified with FTIR analysis. For pellet analysis, 200 mg of potassium bromide was added to each mg sample and powder mixture was compressed to obtain a 15 mm disc in press (Model-C, Carver Inc., IN, USA). FTIR analysis were performed both pellet and ATR mode.

#### **2.2.3.6. Microcomputed Tomography (Micro-CT) Analyses**

Interconnectivity and pore size distribution of HAp microcarriers were examined by Micro-CT (Skyscan 1272, Bruker, Belgium) at BIOMATEN, METU. Micro-CT with a source of 60 kV, a current of 167  $\mu\text{A}$ , and resolution of 26.7  $\mu\text{m}$  was used to acquire X-Ray Radiographs.

### 2.2.3.7. Simvastatin Loading to HAp Microcarriers

Simvastatin (SIM; Sigma, Canada) stock solution was prepared in methanol at a concentration of 1 mg/ml. The stock solution was diluted to different concentrations (0.5, 0.1 and 0.01 mg/ml). 10 mg sintered porous HAp microcarriers were immersed in Simvastatin solutions with four different concentrations (1, 0.5, 0.1 and 0.01 mg/ml) and incubated at 4 °C in refrigerator overnight. After loading, the drug solution was pooled and the microcarriers were frozen at -80 °C. Microcarriers were freeze dried with a freeze dryer (Labconco Freezone 6 Plus, USA). Simvastatin amount in the pooled simvastatin solution was determined by UV-HPLC using calibration curve of simvastatin in 1-50 µg/ml range (Appendix A). The encapsulation efficiency and drug loading of the microcarriers were calculated using the following formulas:

$$\text{Encapsulation Efficiency (\%)} = \frac{\text{Actual Drug Loading}}{\text{Theoretical Drug Loading}} \times 100 \quad (1)$$

$$\text{Drug Loading (\%)} = \frac{\text{Weight of the Drug in Microcarriers}}{\text{weight of Microcarriers}} \quad (2)$$

#### **2.2.3.8. DAT Isolation and Coating of HAp Microcarriers**

Porous microcarriers have a risk of the initial drug burst so that the microcarriers were decided to be coated to slow down the release of SIM in this study. Decellularized adipose tissue (DAT) was chosen for coating because of its fibrillar and collagenous structure. DAT used was isolated from adipose tissue of human donors. Ethical approval for the use of human adipose tissue from healthy female donors was obtained from Human Ethical Committee of Middle East Technical University (See Appendix A). The whole procedure for DAT isolation is shown in **Figure 4**. Lipoaspirates were used with the consent of patients undergoing this procedure. They were firstly washed with PBS for 2 hours and placed in 1% sodium dodecyl sulfate (SDS) for decellularization. The tissue was constantly stirred in SDS solution for 48 hours, washed with dH<sub>2</sub>O and strained. Strained tissue was placed in 2.5 mM sodium deoxycholate in 1X PBS supplemented with 500 units of Porcine lipase and 500 units of porcine colipase (Sigma,USA). After enzymatic digestion for approximately 48 hours, the tissue became visibly white. Digested tissue was rinsed with dH<sub>2</sub>O and finally was frozen at -80 °C overnight. The frozen decellularized tissue (DAT) was subsequently lyophilized and dried. DAT powder was then was milled. For solubilization of DAT, firstly 3200 I.U. porcine pepsin (Sigma, USA) was solubilized in 0.1 M HCl and 1 mg pepsin was added to every 10 mg decellularized tissue. The mixture was digested for 48 hours at room temperature under constant stirring. After 48 hours, pH of the mixture was adjusted to 7.4 using 1 M NaOH. Finally, prepared DAT solution was diluted to 15 mg/ml using 10 X PBS (Young et al., 2011).

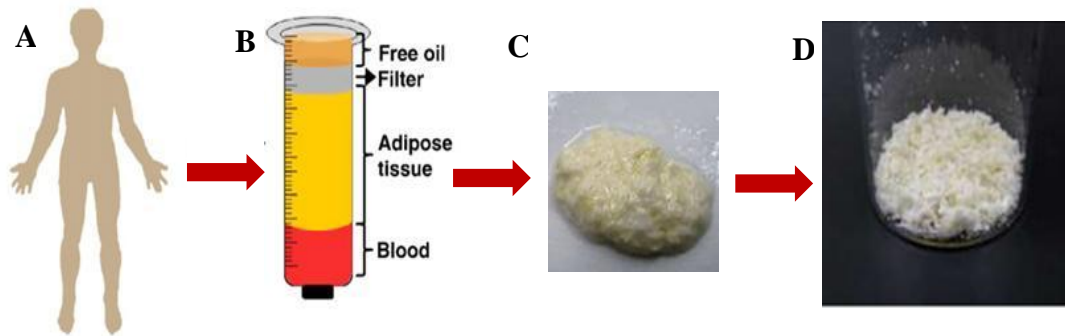


**Figure 4.** Schematic representation of DAT powder isolation: (A) Human adipose tissue were collected from human donor, (B) lipoaspirate were washed PBS to remove blood cells and oil content(C) washed lipoaspirates was enzymatically digested.

After DAT was solubilized with Pepsin/HCl solution, sintered microcarriers were firstly loaded with simvastatin and dried at 4 °C. Dried microcarriers were then immersed into DAT solution at 4 °C and 37 °C, and stored overnight. After removing the DAT solution the microcarriers were dried at room temperature. Morphology of microcarriers before and after DAT coating was studied by field emission scanning electron microscopy (FESEM).

#### **2.2.3.9 *In Vitro* Simvastatin Release From DAT Coated and Uncoated HAp Microcarriers**

Simvastatin release studies from HAp based coated and uncoated microcarriers were conducted in 10 ml PBS (0.1 M pH 7.4) at 37 °C in a shaking water bath (Nüve, Turkey). At pre-defined time points, 1 ml of release medium was collected from release media and replaced with fresh media.

The amount of released simvastatin was determined at 238 nm by UV-HPLC (Reservoir Tray-Shimadzu, Japan) with using calibration curve (n=3) (Appendix A). Inertsil ODS-3 column (250 mm × 4.6 mm I.D. particle size 5 µm) was used at 40 °C and the sample was eluted with a mobile phase consisting of acetonitrile/20 mM Potassium phosphate buffer pH 5.6 (65:35, v/v%) at 30 min at a flow rate 1 ml.min<sup>-1</sup> with 20 µl injection volume. However, SIM amount could not be determined under those release media conditions. In order to determine SIM release kinetics, ethanol included PBS (20:80 v/v) release media and Simulated Body Fluid (1X SBF) were also used.

#### **2.3.4. *In Vitro* Cell Culture Studies**

Human adipose derived stem cells (hASCs) and human Osteosarcoma, Saos-2 (ATCC, USA) cell line, were used for cell culture studies. Cell attachment, proliferation and osteogenic differentiation of cells on HAp microcarriers were studied.

##### **2.3.4.1. Isolation of Human Adipose Derived Stem Cells (hASCs)**

Human adipose tissue was collected from healthy female donors upon receiving approval from Human Ethical Committee of Middle East Technical University (see Appendix A). Lipoaspirates of healthy patients were used with their consents. Tissues were washed with phosphate buffered saline (PBS) to remove blood cells and any contaminants. Washed lipoaspirates were enzymatically digested with 0.075% type IA collagenase (Sigma, USA) in PBS at 37 °C for 40 min. The digested adipose tissue was centrifuged at 1200 g for 5 min. The pellet was then resuspended and filtered with a 100 µm mesh filter to remove residual particles. Isolated cells were seeded in 25 cm<sup>2</sup> culture flasks (Orange scientific, Belgium) at a density of 5 × 10<sup>6</sup> mononuclear cells and cultured in low glucose DMEM, containing 10% FBS and

Penicillin/Streptomycin. After changing the media two days post seeding the adherent cell were cultured at 37 °C in a 5% CO<sub>2</sub> incubator (5215 Shellab, USA) until confluency (Eom et al., 2011). Then, the cells were tyripsinized and expanded until 3<sup>rd</sup> passage. The media were changed twice each week.

#### **2.3.4.2. Cell Attachment and Proliferation Studies**

For cell attachment and proliferation studies hASCs and Saos-2 cells were seeded onto sterilized microcarrier groups in 96 well suspension plates at a density of  $2 \times 10^4$  cells/cm<sup>2</sup>. Cell culture media was refreshed for twice a week. Cells were incubated 37 °C in a 5% CO<sub>2</sub> incubator for 14 days. At pre-defined time points, the media were removed and PrestoBlue<sup>®</sup> was added onto fresh media in a ratio of 1:9 (v/v) and incubated at for 2 h in dark. After incubation, the medium was collected and new media were to each well containing cell seeded microcarriers and incubation of cell seeded microcarriers was continued. The absorbances of pooled aliquots were measured at 570-600 nm by microplate reader (μQuant, Biotek, USA). Percent reduction of the Alamar blue reagent by the cells was calculated according to the formula below. The molar extinction coefficients in the equations are shown in **Table 3**. Abbreviations for the microcarrier groups used in this study are given in **Table 4**.

$$\text{Percent Reduction of PrestoBlue™ Reagent} = \frac{(O_2 \times A_1) - (O_1 \times A_2)}{(R_1 \times N_2) - (R_2 \times N_1)} \times 100 \quad (3)$$

Where:

O<sub>1</sub>=molar extinction coefficient of oxidized PrestoBlue™ reagent at 570 nm

O<sub>2</sub>=molar extinction coefficient of oxidized PrestoBlue™ reagent at 600 nm

R<sub>1</sub>= molar extinction coefficient of reduced PrestoBlue™ reagent at 570 nm

R<sub>2</sub>= molar extinction coefficient of reduced PrestoBlue™ reagent at 600 nm

A<sub>1</sub>=absorbance of test wells at 570 nm

**Table 3.** Molar Extinction Coefficients of PrestoBlue™ Reagent.

<b>Wavelength</b>	<b>Reduced (R)</b>	<b>Oxidized (O)</b>
<b>570 nm</b>	155677	80586
<b>600 nm</b>	14652	117216

**Table 4.** Experimental Groups and Their Abbreviations.

Experimental Groups	Abbreviations
HAp microcarriers	HAp
DAT coated HAp microcarriers	DAT-HAp
HAp microcarriers loaded with 0.5 mg/ml SIM	HAp-0.5
DAT coated HAp microcarriers loaded with 0.5 mg/ml SIM	DAT-HAp-0.5
HAp microcarriers loaded with 0.1 mg/ml SIM	HAp-0.1
DAT coated HAp microcarriers loaded with 0.1 mg/ml SIM	DAT-HAp-0.1
HAp microcarriers loaded with 0.05 mg/ml SIM	HAp-0.05
DAT coated HAp microcarriers loaded with 0.5 mg/ml SIM	DAT-HAp-0.05

#### **2.3.4.3. *In Vitro* Differentiation Studies**

Osteogenic differentiation of Saos-2 (ATCC, USA) was conducted by Alkaline phosphatase Activity Assay (Sigma, USA). Cells were seeded onto microcarriers into 96 well suspension plates at a density of  $2 \times 10^4$  cells  $\text{ml}^{-1}$ . Cells were incubated in osteogenic medium (DMEM supplemented with 10% FBS, antibiotic, 50  $\mu\text{g}/\text{ml}$  ascorbic acid, 10 mM  $\beta$ -Glycerophosphate and  $10^{-8}$  Dexamethasone) for 14 days. Medium of each plate were refreshed twice a week. At days 7 and 14, the cells were

rinsed with PBS, fixed with 4% formaldehyde, dehydrated with an increasing ethanol concentration. They were then dried after dipping in hexamethyldisilazane.

#### **2.3.4.4. Microscopical Examinations**

The morphology of the cells on microcarriers, which were incubated in growth media or osteogenic differentiation media, was studied by SEM examinations. The cells were fixed with 4% formaldehyde, dehydrated with an increasing ethanol concentration and dried after dipping in hexamethyldisilazane. The specimens were coated with gold in vacuum environment before SEM (FEI Quanta 400F, USA) analyses using a sputtering equipment. The proliferation and penetration of cells into the pores of microcarriers were also investigated with Confocal Laser Scanning Microscopy (CLSM, Zeiss LSM 510). At different time points, cells were fixed with 4% paraformaldehyde solution in PBS and were permeabilized with Triton X-100. Cells were stained with Propidium iodide and Phalloidin-FITC for nucleus and cytoskeleton, respectively and samples were observed by using long distance objectives, laser and phase contrast methods. For visualization of the migration of attached cells into pore channels z-stack images were captured by Zeiss LSM 510 confocal laser scanning microscopy.

## CHAPTER 3

### RESULTS AND DISCUSSION

#### 3.1. Characterization of HAp Powders

##### 3.1.1. XRD Analyses of HAp Powders

Pure HAp powders were synthesized by both co-precipitation and sol-gel methods for the preparation of HAp based microcarriers. The details of the synthesis methods are given in Chapter 2. **Figures 5(a) and 5(b)** show the XRD patterns of the amorphous and calcined HAp powders by co-precipitation and sol-gel methods, respectively. Note that the spectra of as-prepared (denoted as amorphous) samples in **Figure 5** refer to powders prepared by co-precipitation and sol-gel methods, respectively without a further calcination process. The standard diffraction peaks from random HAp crystals (Joint committee on Powders Diffraction Standards, card no 9-0432), are also given for comparison at the bottom of **Figure 5(a)**. Based on the standard, there were no significant impurities or secondary phases in as-prepared and calcined powders regardless of the synthesis method. In addition, all samples exhibited the strongest peaks between 30-35° and the relative ratio of peak intensities for all samples were in accordance with the standard reflection, hence indicating that the crystals showed no preferred orientation (randomly oriented polycrystals). The crystallinity of the co-precipitated powders was significantly higher than sol-gel processed samples as evidenced from the peak intensities regardless of whether the sample was in the as-prepared or calcined state. This is expected; since the reaction kinetics of crystallization and growth during precipitation is probably much higher

and difficult to control compared to sol-gel method used in this study. During precipitation, precipitated powders grow in size and agglomerate while newly nucleated crystals continue to precipitate. On the other hand, crystallization and particle growth occur more or less simultaneously and homogeneously for sol-gel prepared powders during calcination step. More importantly, as explained in Section 2.2.1, the solution temperature during precipitation was  $\sim 60$  °C whereas the solution in sol-gel method was kept at room temperature. This also clearly suggests that the reaction kinetics is enhanced for the precipitation process. As a consequence, although the as-prepared powders had lower crystallinity, peak intensities were still higher compared to sol-gel prepared powders. Keeping in mind the calcination time and temperature are identical for both processes, high crystallinity of precipitated powders in **Figure 5** is expected based on the above mentioned discussion. It has been shown that powders with lower crystallinity exhibit higher *in vitro* dissolution rates (Cai et al., 2007), because atomic bonds in a perfect crystal are much stronger than their amorphous counterparts, which leads to enhanced chemical resistivity and lower reactivity for crystalline materials. From this point of view, the high crystallinity of precipitated powders might be advantageous. This is due to the mechanical stability is increased with high crystallinity (Champion, 2013). The complementary particle size discussion is provided in the proceeding sections.

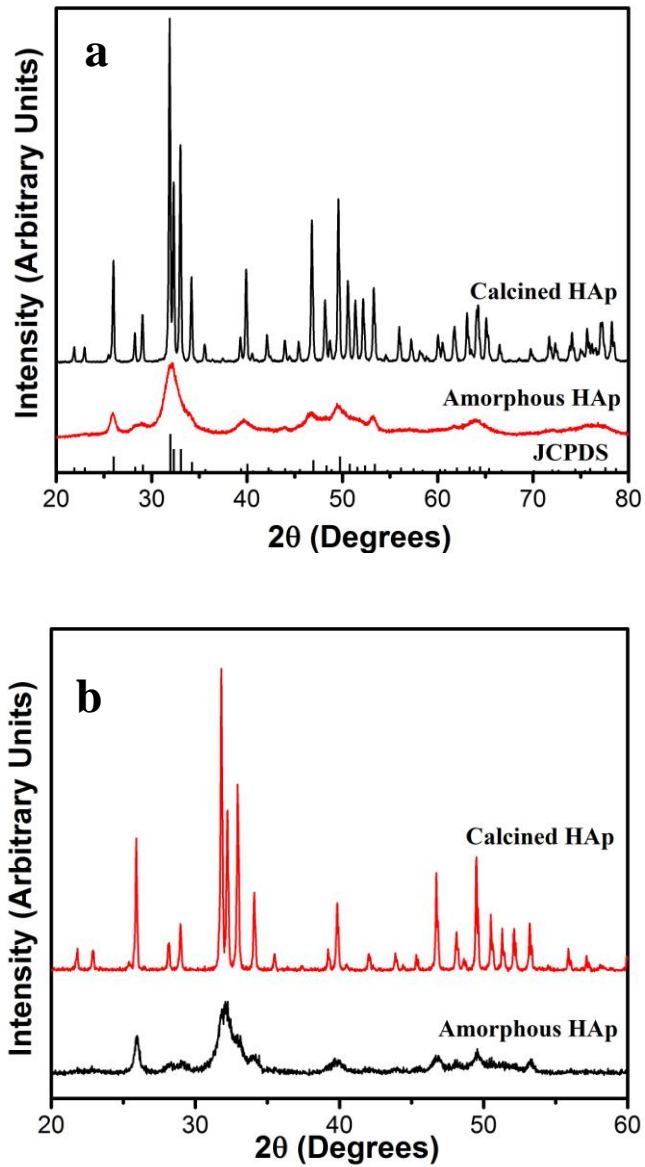


**Figure 5.** XRD patterns of calcined and as synthesized (amorphous) HAp powders prepared by (a) co-precipitation and (b) sol-gel methods. Joint committee on Powders Diffraction Standard (JCPDS) data for HAp crystals are shown for comparison.

XRD patterns of commercial Nano-HAp powders and HAp based microcarriers prepared from these powders are illustrated in **Figure 6**. It can be seen that the peaks are slightly more widened for Nano-HAp, which indicate powders with smaller particle size compared to calcined microcarriers (Pattanayak et al., 2010). Moreover, there were no additional peaks in the spectrum of the calcined microcarriers indicating phase purity of powders is maintained.

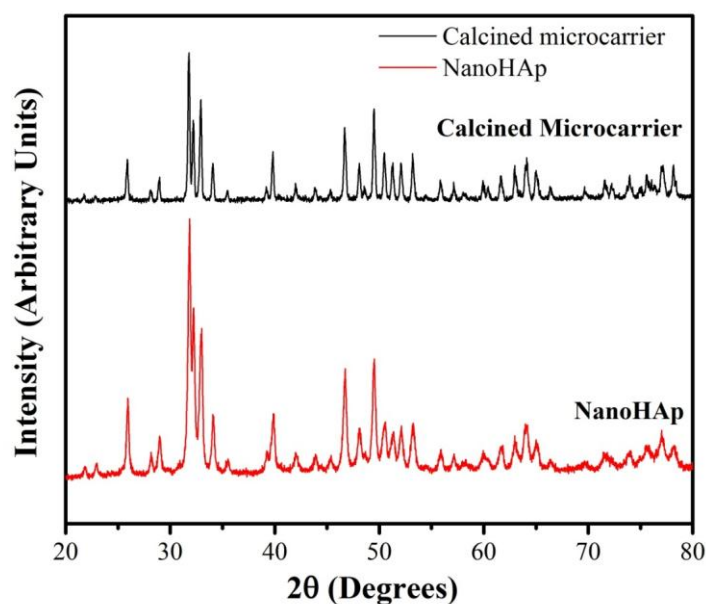


**Figure 6.** XRD patterns of Nano-HAp and sintered Nano-HAp based microcarriers.

### 3.1.2. Scanning Electron Microscopy Analyses

SEM images of amorphous (as-synthesized) sol-gel based and precipitated HAp powders are shown in **Figure 7**. It was observed that HAp particles were agglomerated even after grinding and they had a broad particle size distribution. The average particle sizes of sol-gel and precipitated powders obtained by measuring particle sizes from SEM examinations are  $10.31 \pm 12.85$  and  $12.39 \pm 16.88\mu\text{m}$ , respectively. It should be noted that precipitated powders showed a much wider

particle size distribution compared to sol-gel powders which can also be inferred from the larger standard deviation of the measurements. This observation is expected because of the high reaction kinetics involved in the precipitation method in this study and explained previously in Section 3.1.1. Both powders were not suitable for microcarrier preparation because of their large particle sizes and wide size distributions. This issue is addressed in the next section and it will be shown that the use of Nano-HAp powders is actually necessary to form spherical microcarriers in the desired size range.

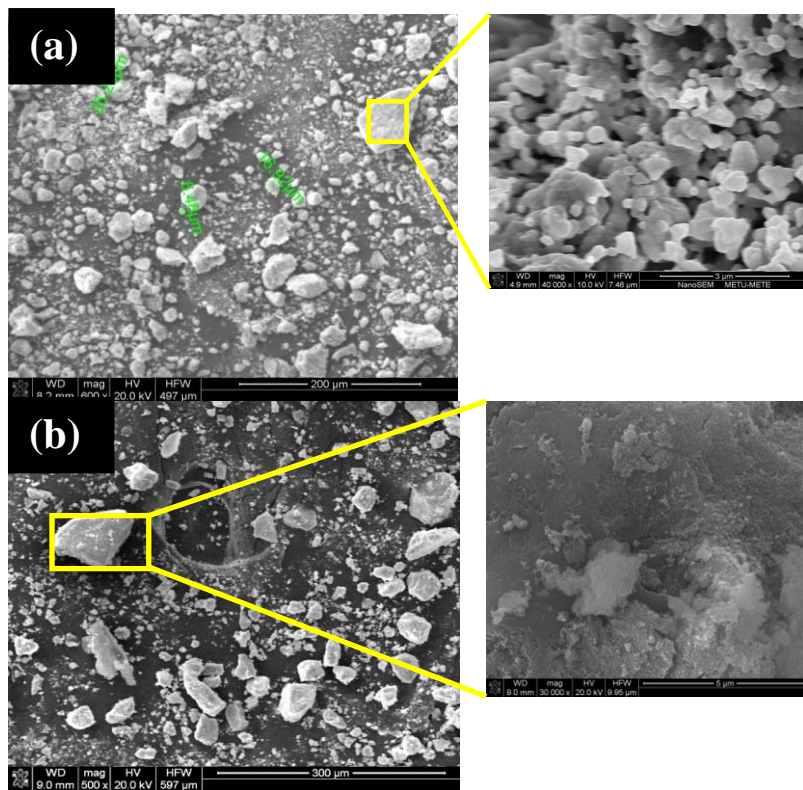


**Figure 7.** SEM images of amorphous HAp powders synthesized by (a) sol-gel and (b) co-precipitation methods.

### 3.2. Optimization of HAp Based Microcarrier Preparation

In this study, HAp powders were used for the preparation of microcarriers. HAp powders and hydrophobic camphene oil were mixed for providing a homogenous porous structure to HAp microcarriers. Camphene, a crystalline plastic at room temperature, has been used in recent studies as a porogen (Yang et al., 2011; Yoon et al., 2007). Its melting point is approximately 44-48 °C. It has been reported that camphene forms dendrites when it solidifies (Araki and Halloran, 2005). After solidification, the surfactant and ceramic powder mixture provides a barrier to camphene. Therefore, interconnected pore structure was obtained when it was sublimated. Gelatin, a natural polymer, was chosen as a binder component for the microcarrier preparation.

During the optimization studies of microcarrier preparation, the effects of particle size of the starting HAp powders, the effects of concentration and type of the surfactant on morphology and pore structure of the carriers were examined. The choice of surfactants highly affects the final pore morphology of microcarriers because of their different molecular structures (Francis et al., 2011). Firstly, microcarriers were prepared with the co-precipitated HAp powders. Two different surfactants (SDS, Tween-20) were used to prepare the microcarriers in this study and morphology and pore structures of the obtained microcarriers were compared with respect to SEM images in **Figure 8**.

**Figure 8** shows the SEM images of microcarriers with and without surfactants. As seen, surfactants were highly effective for the formation of spherically-shaped microcarriers and the type of surfactant determines the final morphology of the carrier. From **Figure 8(a)** and **8(b)**, the spherical shape of microcarriers prepared with SDS and Tween-20 was much better than the carriers prepared without any surfactant in **Figure 8(c)**. Microcarriers prepared using SDS as dispersant had a more compact structure without showing any disintegration compared to those prepared with Tween-20. However, porosity was low and the pore size distribution on the

surface was wide. However, porous and compact microcarrier structures with load-bearing capability could not be achieved.

According to SEM images, it can be inferred that the surfactant was not the only factor that affects porosity. Slurry mixture must also be homogeneously mixed to ensure formation of perfectly spherical carriers with a uniform pore size distribution on the surface. Viscosity of such mixtures is determined from powder characteristics including specific surface area, size of the powders and the agglomeration state which are crucial for the formation of ideal microcarriers with high surface reactivity (Lee et al, 2007). The effect of dispersants on the morphology of powders was examined from the SEM images. Microcarriers were frozen at -20 °C and lyophilized. The frozen camphene formed branched tree structures inside of the microcarriers after freezing. These dendritic structures served as templates and were replaced with pore channels after sublimation (**Figure 8**).

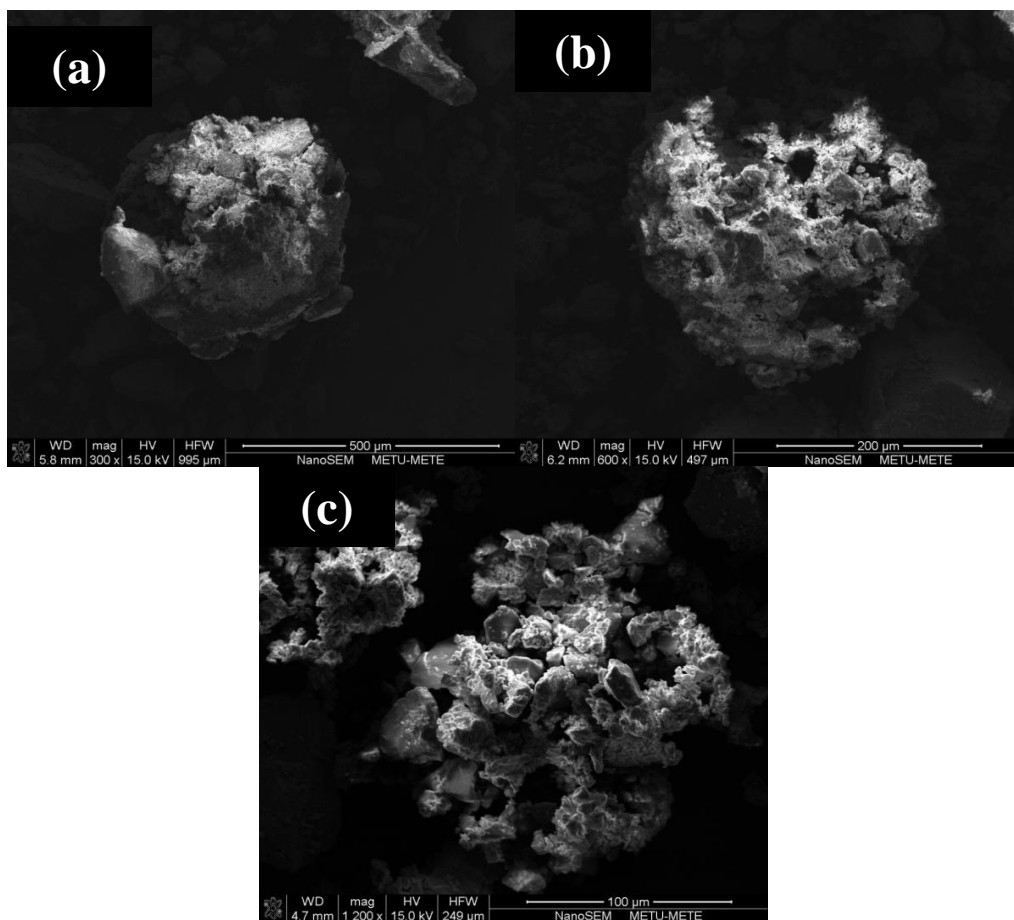


**Figure 8.** SEM images of microcarriers prepared with co-precipitated HAp and different surfactants: (a) SDS, (b) Tween 20, and (c) surfactant free.

**Figure 9** shows the images of microcarriers synthesized using different HAp starting powders. Among them, the one prepared with Nano-HAp powders in **Figure 9(a)** had a perfect spherical structure. In addition, these carriers had lower tendencies to split up and their condense/compact structures were maintained. However, there were few open pores on the surface, which make them unsuitable for drug loading/release and also for cell attachment. **Figure 9** clearly shows that the size of the starting powder is critical to achieve microcarriers suitable for cell and drug delivery where small spherical powders are essential for forming a compact sphere. Surface morphology of Nano-HAp based microcarriers is shown in **Figure 9(a)**. These microcarriers had a compact surface and a perfect spherical shape. It should be emphasized that not only the size of the HAp powders, but also the shape of the powders is crucial to obtain microcarriers with desired properties. For instance, **Figure 9(b)** shows that cracks are formed on the surface of the microcarrier prepared by sol-gel based powder after calcination. Few and uncontrolled open pore structure can be clearly seen in the SEM images. Additionally, **Figure 9(c)** demonstrates that the shapes of the powders were irregular and non-uniform. When they agglomerate during formation of the microcarriers, it becomes very difficult to form a spherical shape, as expected in **Figure 9(c)**.

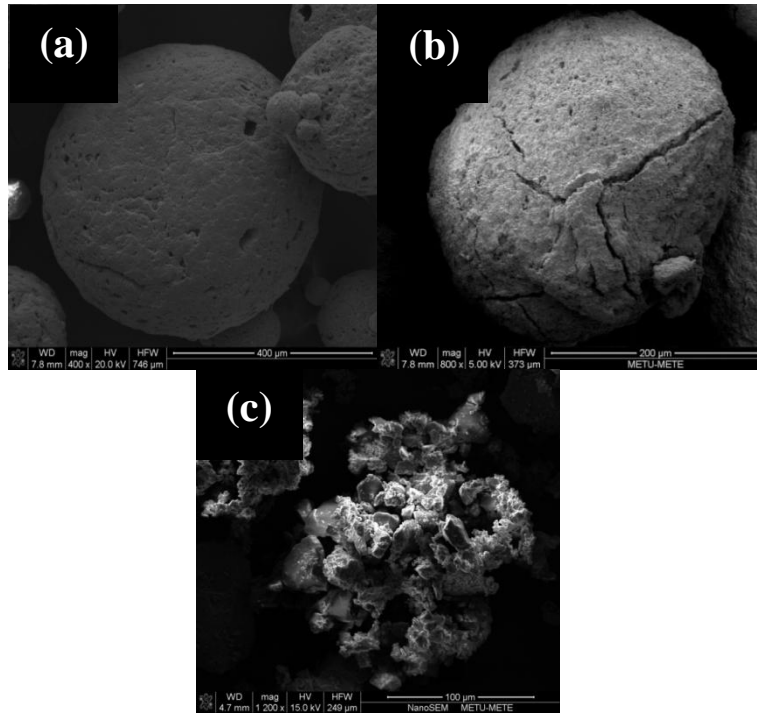


**Figure 9.** SEM images of microcarriers prepared with different sized HAp powders (a) commercial Nano-HAp based (<200 nm), (b) synthesized by sol-gel method and (c) synthesized by co-precipitation method.

Colloidal dispersion is a common ceramic processing approach for controlling the microstructure of the product. Dispersants are used for the regulation of pore structures and introducing interconnectivity in ceramic bodies. In this study, D-3005 was used as a ceramic dispersant for providing interconnected, open-porous microstructure to Nano-HAp microcarriers. D-3005 disperses ceramic powders in water slurry (Yang et al., 2011). It is also an appropriate choice for the gelatin binder due to its solubility in water. The effect of dispersant concentration on the physical properties of microcarriers such as carrier size, porosity and shape was investigated using different amounts of Duramax D-3005. Porosity of the microcarriers is increased with increasing dispersant concentration as seen in **Figure 10(b)** and **10(d)**. This is expected because dispersants are used for decreasing the viscosity of the ceramic/water slurry and stabilize the ceramic in the colloidal dispersion.

However, the optimum dispersant concentration is important to have uniform shaped samples (Fadli, Sopyan, Mel, & Ahmad, 2011). The excess amount of dispersant leads to reagglomeration during emulsion step as seen in **Figure 10(a)** and **10(b)** for the microcarriers with 0.5% Duramax. Although the spherical shape of the individual microcarriers was somewhat maintained using 0.4% Duramax, the carriers showed large degree of agglomeration. It has been reported that the concentration of polymeric bridging of polyelectrolytes higher than the critical amount leads to an increase in particle sizes of the ceramic body due to their polymeric bridging (Fazio et al., 2008). This probably increases the viscosity of the slurry and as a result, the agglomerated clusters form nonporous and rod-like structures for slurries with the highest concentration of Duramax as shown in **Figure 10(a)**.

**Figure 11** shows that the pore sizes of the carriers significantly increased when ceramics were prepared with a suitable dispersant concentration. The mean size of HAp microcarriers prepared by Nano-HAp was determined to be 426  $\mu\text{m}$  (**Figure 12**). Microcarriers that are above 100  $\mu\text{m}$  and less than 850  $\mu\text{m}$  are generally used as bone grafts (Bohner et al., 2013). In **Figure 13**, 3D micro-CT images show that the microcarriers had interconnected pores with connected through channels.

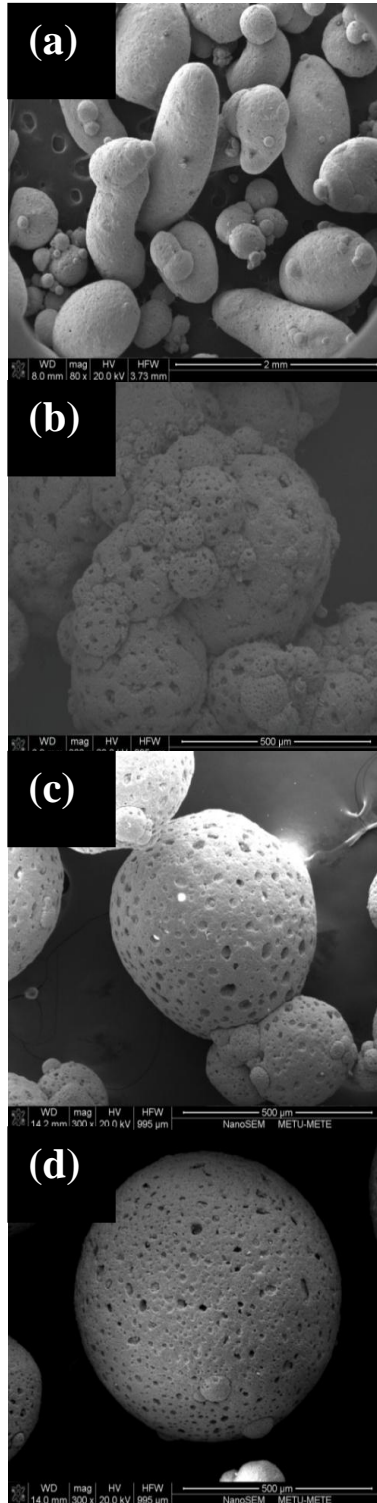


**Figure 10.** SEM images sintered microcarriers prepared with (a) 0.5% (b) 0.4% (c) 0.35% and (d) 0.3% Duramax D-3005 dispersant.

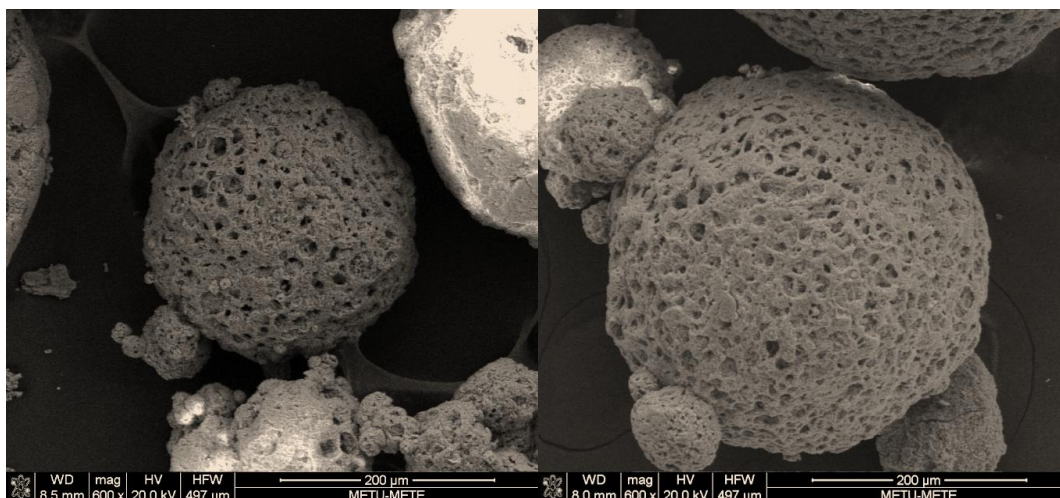


**Figure 11.** Nano-HAp based microcarriers prepared with water in oil (w/o) emulsion method using 0.3% D-3005 as dispersant.

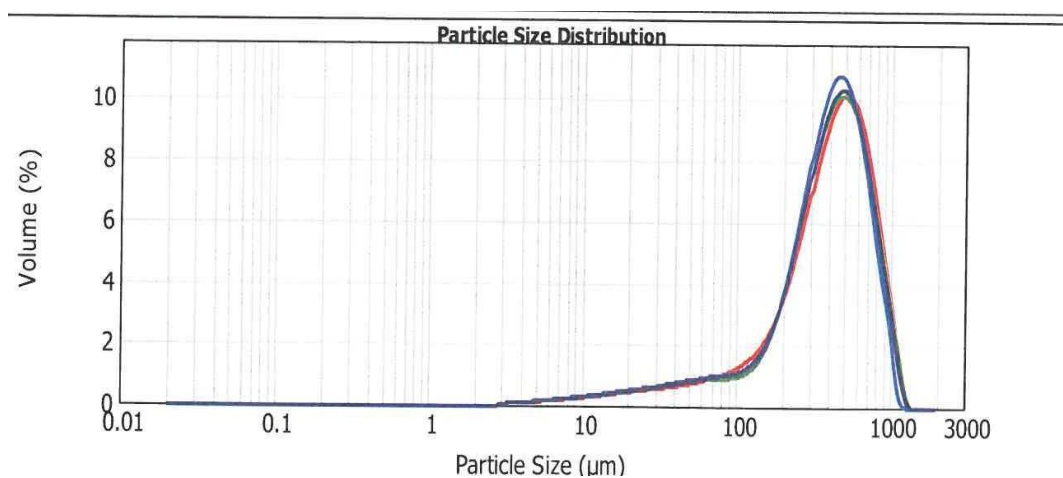


**Figure 12.** Particle size distribution histograms of Nano-HAp based microcarriers prepared by w/o emulsion method.

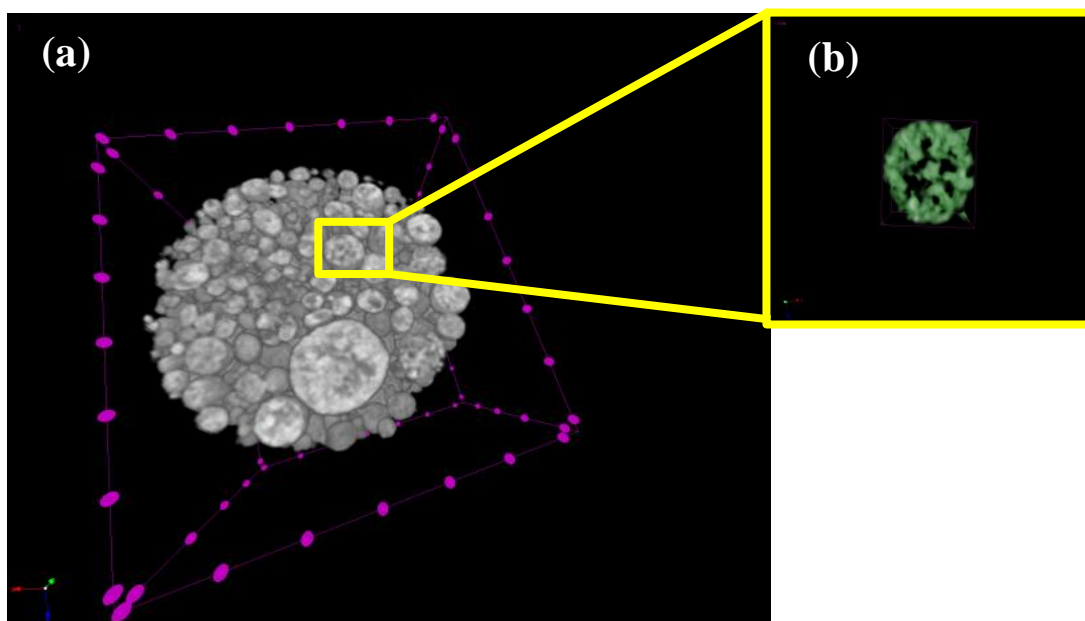


**Figure 13.** 3D images of (a) Microcarriers in Eppendorf after Micro-CT scanning and (b) cross-sectional scanning of single microcarrier.

### 3.2.1. Characterization of DAT Coated Microcarriers

In this study, the aim was to obtain a delivery system that can provide similar structure and properties with hard tissue and have a potential for encapsulating drugs and releasing them in a controlled way. First step was the preparation of porous HAp based microcarriers. The prepared microcarriers had a highly porous structure with interconnected channels; however drug loading to a porous structure was a drawback. Burst release of the drug can cause toxicity related problems. Considering the hard tissue organic-inorganic matrix structure, for controlling the drug release, human derived DAT were used. For the coating process, sintered microcarriers were immersed in DAT tissue solution prepared in 0.1 M pepsin/HCl with every 10 mg DAT powders. Gelation of DAT matrix onto microcarriers was performed by

incubating in DAT solution at 4 °C and 37 °C overnight. **Figure 14** shows the SEM images of microcarriers coated at two different temperatures.

As seen from **Figure 14(a)**, microcarriers were coated with a thin shiny layer of DAT. However, Pati et al., showed that gelation ability of DAT tissue started to increase beyond 15 °C and significantly increased when the temperature was 37 °C (Pati et al., 2014). Therefore, gelation was tried at 37 °C in our study to obtain a stable coating structure. **Figure 14(b)** shows that DAT coated at 37 °C covered the microcarriers and provided a rougher surface for the cells to attach easily onto DAT coated microcarriers (Young et al., 2012).

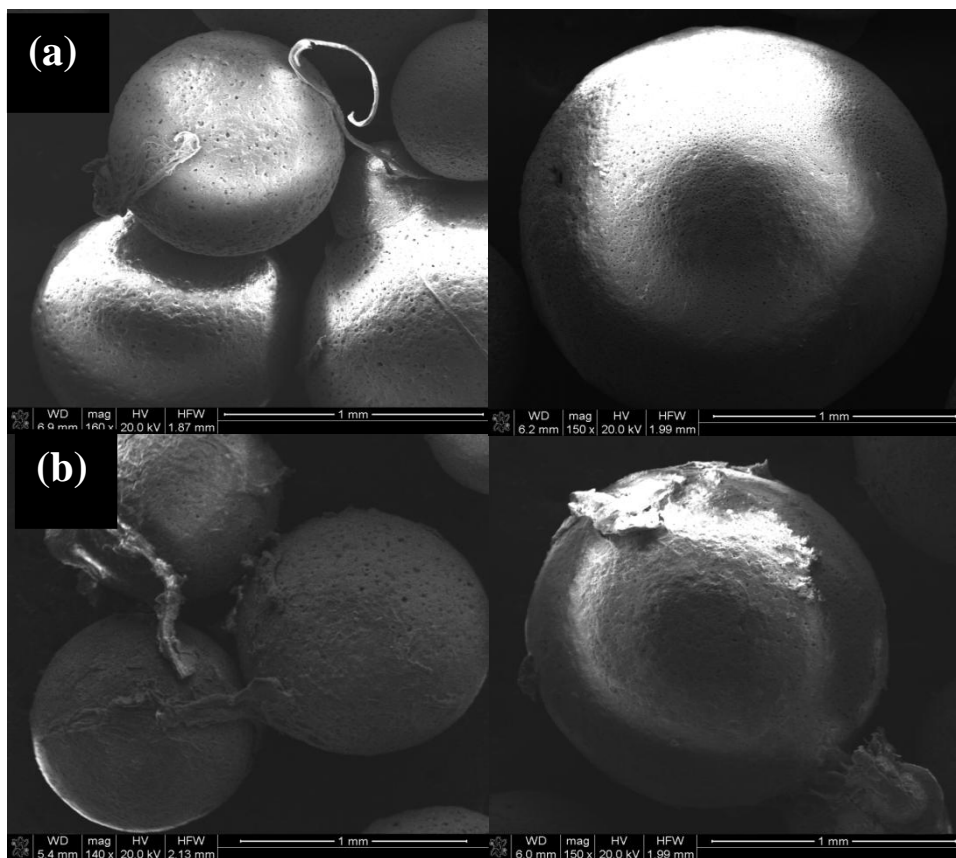


**Figure 14.** SEM images of DAT coated microcarriers at (a) 4 °C and (b) 37 °C.

### 3.3. Simvastatin Loading and Encapsulation Efficiency

Microcarriers were loaded with SIM with solvent immersion method using 1, 0.5, 0.1 and 0.01 mg/ml drug stock solutions. Microcarriers were immersed into SIM solution prepared in methanol and loading was carried out at 4 °C for overnight. Loaded drug amount in the drug solution removed after overnight incubation was determined by UV-HPLC. The loading experiments were conducted by using two different amounts of microcarriers and their encapsulation efficiencies are given in **Table 5**. In the first loading experiment, 20 mg microcarriers were immersed in 1 ml stock SIM solutions

in methanol with different concentrations (1, 0.5 and 0.1 mg/ml corresponding to 2389.14, 1194.57 and 238.91  $\mu\text{M}$ ), respectively) and the initial drug amount encapsulated in microcarriers were 59%, 61% and 32%, respectively. Zhou et al. prepared an injectable tissue-engineered bone (ITB) composed of human adipose-derived stromal cells (hADSCs) and platelet-rich plasma (hPRP) and different concentrations of SIM in the range of 1 nM-10  $\mu\text{M}$ . They showed that 2  $\mu\text{M}$  ( $\sim 8.37 \times 10^{-7}$  g/mL) and higher amounts of SIM slowed down the cell growth and proliferation when injected to bone. The group reported that 1  $\mu\text{M}$  was optimal SIM concentration for local bone applications (Zhou et al., 2010). Due to toxicity concerns, 1 mg/mL stock solution was not used in our study (**Table 5**). Additionally, there can be a saturation level of microcarriers for drug loading, which might cause lower loading of SIM into the microcarriers. As a result, the amount of microcarriers for further SIM release studies was increased to 50 mg and they were loaded with 0.5 and 0.1 mg/mL SIM (**Table 5**). Drug loading for stock 0.01 mg/mL could not be determined since the loaded SIM was not in detectable range by HPLC. Microcarriers loaded with 10 mg/ml SIM were examined using FTIR in the range of 4000 and 2000  $\text{cm}^{-1}$  wavenumbers. FTIR spectroscopy was used to examine the possible interactions between SIM and hydroxyapatite microcarriers after physical drug loading process (Wu et al., 2014). **Figures 15** and **16** show the FTIR spectra of SIM loaded and SIM-free microcarriers. Characteristic bands of SIM were observed only in HAp microcarriers loaded with 10 mg/ml SIM stock solution. The microcarriers with highest SIM content showed similar bands to those observed in pure SIM at 2955.04 and 2872.10  $\text{cm}^{-1}$  (Alkene C–H stretching vibrations) (Amsa et al., 2014) (**Figure 15**). Characteristic bands of HAp were also observed 1041 $\text{cm}^{-1}$  and 570  $\text{cm}^{-1}$  assigned to  $(\text{PO}_4)^{3-}$  groups (**Figure 16**).

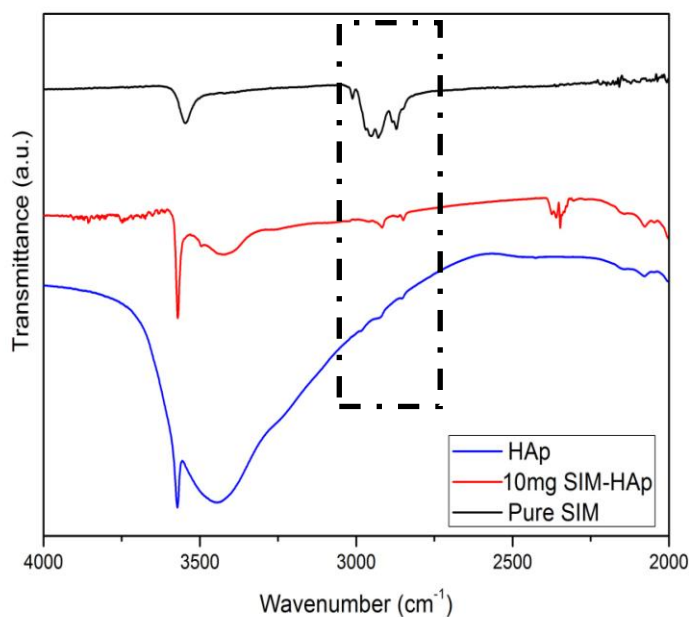


**Figure 15.** FTIR spectra of pure SIM and SIM free and SIM loaded HAp microcarriers in 4000-2000 cm<sup>-1</sup> range. Arrows at wavenumbers 2955 and 2872 cm<sup>-1</sup> are assigned to C-H stretchings of SIM.

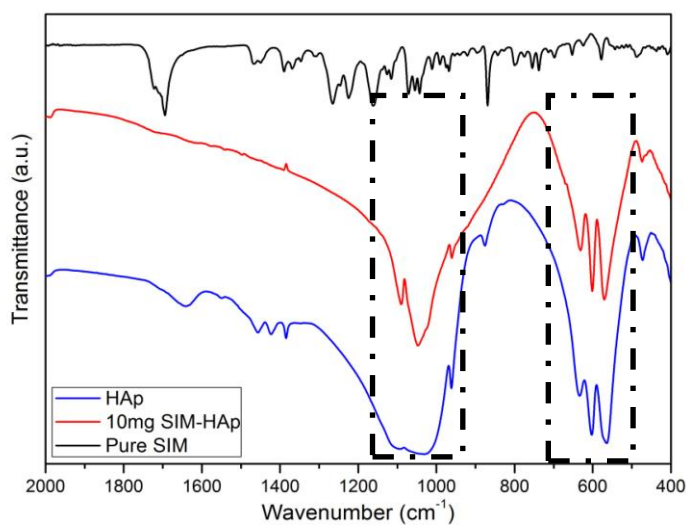


**Figure 16.** FTIR spectra of pure SIM, SIM free and SIM loaded HAp microcarriers in 2000-400 cm<sup>-1</sup> range. Dashed boxes show the mean (PO<sub>4</sub>)<sup>3-</sup> bands.

**Table 5.** SIM loading and encapsulation efficiencies of HA microcarriers (n=4).

<b>Stock Solution (<math>\mu\text{g/mL}</math>)</b>	<b>Drug Loading (<math>\mu\text{g drug/mg}</math> microcarriers)</b>	<b>Encapsulation Efficiency (%)</b>	<b>The amount of microcarriers (mg)</b>
<b>1000</b>	$29.51 \pm 1.36$	$59 \pm 2.72$	20
<b>500</b>	$15.18 \pm 0.80$	$61 \pm 3.23$	20
<b>100</b>	$1.64 \pm 0.41$	$32 \pm 8.2$	20
<b>500</b>	$4.52 \pm 0.12$	$34 \pm 6.27$	50
<b>100</b>	$0.045 \pm 0.01$	$45 \pm 1.76$	50

### **3.4. *In Vitro* Release Profiles of SIM Loaded Microcarriers**

In order to study the release profiles of SIM loaded microcarriers, 20 mg microcarriers with loadings of 1.64, 4.52 and 0.045  $\mu\text{g drug/mg}$  (**Table 5**) were immersed in 10 ml PBS, pH 7.2 in a dialysis tube. Samples were collected at different time points namely 1, 6, 24, 72, 120 and 144 hours. The amount of SIM released could not be determined which could be due to amounts released were lower than the detectable range with HPLC. The amount of microcarriers added to release media was increased to 50 mg and release media were decreased to 5 ml. However, SIM amounts could not be determined. In literature, it was reported that bioceramic based micro or nanospheres that was loaded with drugs such as bisphosphonate, simvastatin or gentamicin show relatively slow local release for extended periods (Nissan, 2014). Chou et al. also reported the results of release study in SBF solution of SIM loaded  $\beta$ -TCP particles (prepared using 4 mg/ml stock solution). The authors obtained the amount of drug release by measuring absorbances with a UV-spectrophotometer (Chou et al., 2013). The solubility of SIM was reported to be

0.0013 mg/ml at 25 °C (Serajuddin et al., 1991). This hydrophobic drug has a very poor solubility in aqueous media. In order to study the release profiles of SIM delivery systems, several modifications were performed for enhancing the solubility of the drug such as increasing the initial loading concentration of SIM. For modification of release media, studies reported that SDS or ethanol can be added to the release media (Diramio, et al., 2008). Regarding the solubility of SIM in ethanol, release media were prepared as ethanol and PBS buffer (20:80 v/v). However, SIM released could not be determined by HPLC or UV spectrophotometry. It was thought that the drug loading and the amount of microcarriers used in the release studies were too low so the amount of drug released could not be determined. For studying the release profile of SIM drug loading, the amount of microcarriers can be increased.

### **3.5. *In Vitro* Cell Culture Studies**

#### **3.5.1. Proliferation of Cells on HAp Based Microcarriers**

The main problem for hydrophobic drugs is their low bioavailability and side effects when administrated at high doses (Roberts and Zhang, 2013). Simvastatin, an osteoporotic drug, whose osteogenic potential has been also shown on stem cells, is a hydrophobic drug with such concerns (Lupattelli et al., 2004). In this study, we aimed to develop SIM loaded HAp microcarriers for bone tissue engineering applications. In order to see the effect of released SIM amount on viability of cells, DAT coated and uncoated HAp microcarriers were cultured with ASCs and Saos-2 cells for 10 days. Presto Blue assay was used to study the proliferation of hASCs and Saos-2 cells seeded onto microcarriers. Initial seeding density was same for both cell types (25000 cell/ cm<sup>2</sup>). In the first day of the incubation period, the percent reduction values varied among groups for Saos-2 cells (**Figure 17**). Higher cell attachment on DAT coated microcarriers was observed compared to uncoated ones. The lowest cell attachment was observed for HAp-0.5, which could be due to higher amount of SIM release from uncoated HAP-0.5 microcarriers. However, such result

was not observed for hASCs cells and the percent reduction values were similar for these cells among all groups on day 1 (**Figure 18**). This could be due to cell type or seeding errors. In general, a time dependent increase in cell number of Saos-2 cells was observed in all groups. Such time dependent increase was also not observed for hASCs. Percent reduction values remained approximately same, pointing out that these cells did not proliferate much upon seeding. For all microcarriers, SIM loadings were all at cytotoxic level. However a time dependent increase in percent reduction was observed indicating that cells proliferated on the microcarriers.

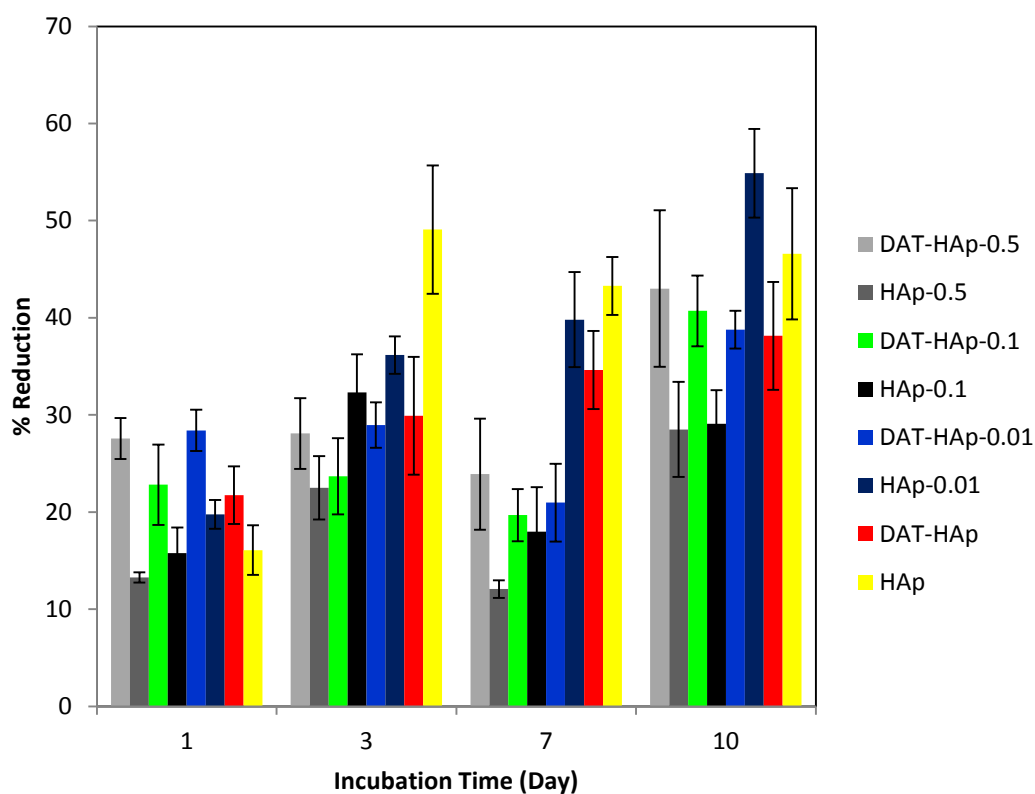


**Figure 17.** Cell proliferation of Saos-2 cells on microcarriers. The groups were: HAp microcarriers (HAp), DAT Coated HAp microcarriers (DAT-HAp), HAp microcarriers loaded with 0.01 mg/ml SIM (HAp-0.01), DAT coated HAp microcarriers loaded with 0.01 mg/ml SIM (DAT-HAp-0.01), HAp microcarriers loaded with 0.1 mg/ml SIM (HAp-0.1), DAT coated HAp microcarriers loaded with 0.1 mg/ml SIM (DAT-HAp-0.1), HAp microcarriers loaded with 0.5 mg/ml SIM (HAp-0.5), DAT coated HAp microcarriers loaded with 0.5 mg/ml SIM (DAT-HAp-0.5).

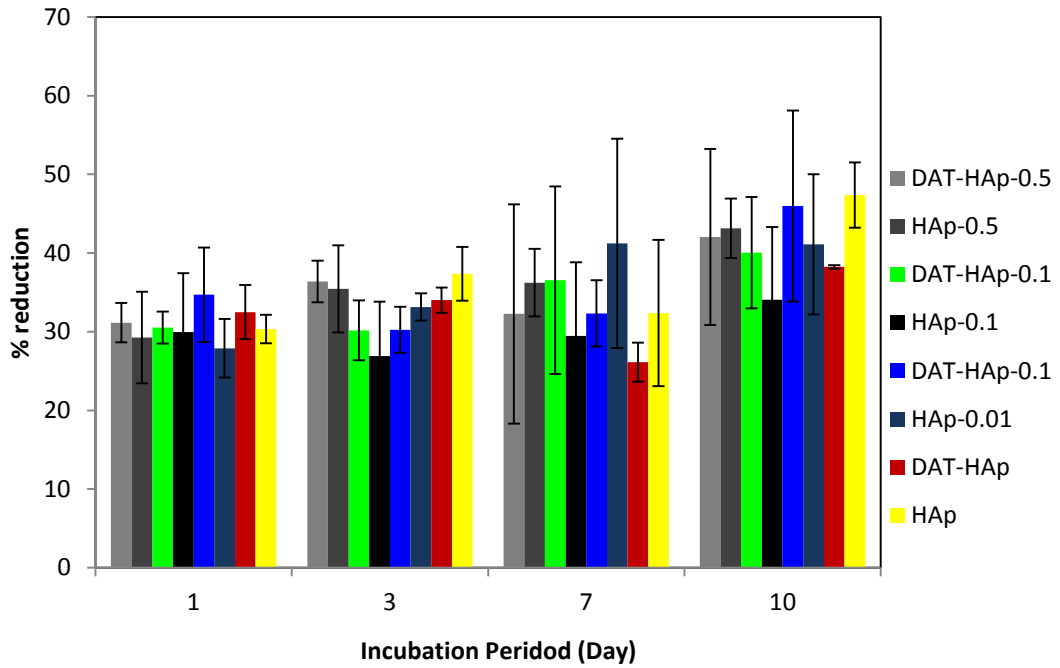


**Figure 18.** Proliferation of ASCs on HAp based microcarriers in growth media. Experimental groups were hydroxyapatite (HAp), DAT coated HAp microcarriers (DAT-HAp), HAp microcarriers loaded with 0.01 mg/ml SIM (HAp-0.01), DAT coated HAp microcarriers loaded with 0.01 mg/ml SIM (DAT-HAp-0.01), HAp microcarriers loaded with 0.1 mg/ml SIM (HAp-0.1), DAT coated HAp microcarriers loaded with 0.1 mg/ml SIM (DAT-HAp-0.1), HAp microcarriers loaded with 0.5 mg/ml SIM (HAp-0.5), DAT coated HAp microcarriers loaded with 0.5 mg/ml SIM (DAT-HAp-0.5).

### 3.5.2. SEM Analyses of Cell Seeded HAP Based Microcarriers

Studies showed that the attachment of the cells on materials varies with surface characteristics and topography of the materials. On the other hand, higher cell attachment was observed on biological materials like DAT coated carriers or scaffolds and cells spread on these scaffolds (Fiedler, et al., 2001). From SEM images it was found that higher ASCs attachment was observed compared to Saos-2 cells (Figures 19 and 20). Saos-2 cells did not form a lawn of cells on the microcarriers. From these images it was observed that microcarriers seeded with hASCs were covered with cells. This was also in agreement with the finding that cells did not increase in number for these cells. This coverage difference could be the size difference between these two cell types since percent reduction values were similar at the same incubation periods.

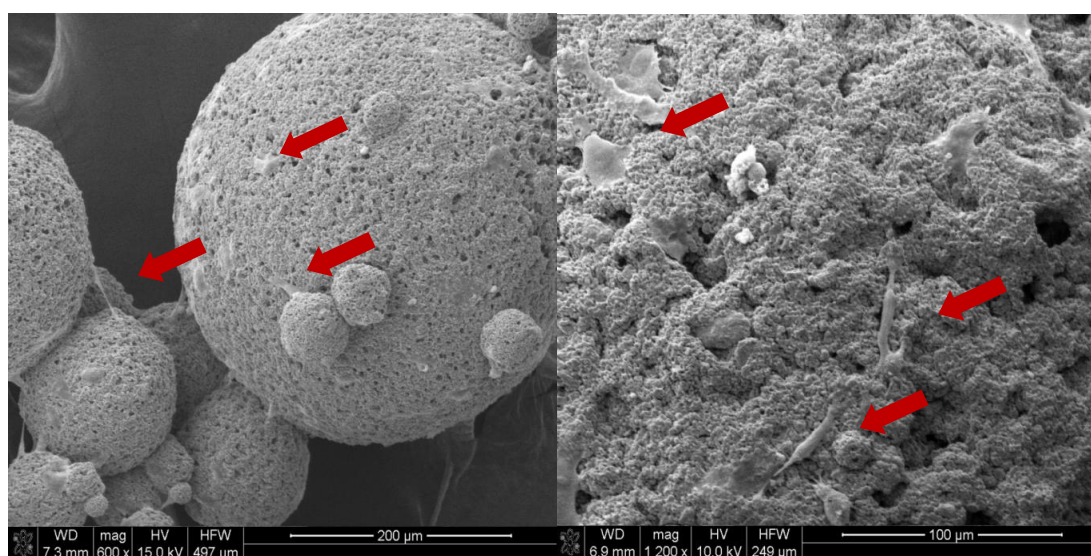


**Figure 19.** SEM images of Saos-2 cell seeded microcarriers after 24 hours of incubation Cells are shown by arrows.

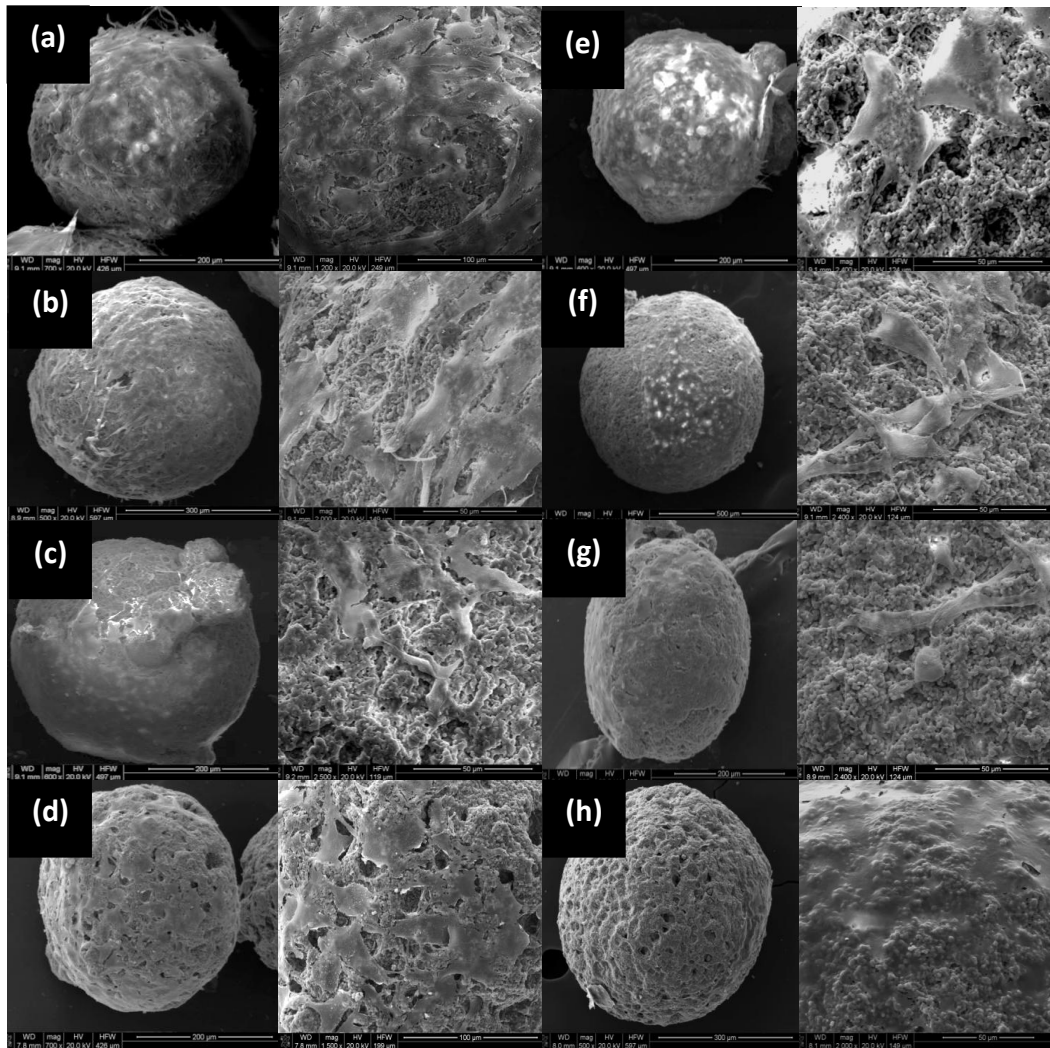


**Figure 20.** SEM images of ASCs seeded on (a) DAT-HAp-0.5 (b) DAT-HAp-0.1 (c) DAT-HAp-0.01 (d) DAT-HAp (e) HAp-0.5 (f) HAp-0.1 (g) HAp-0.01 (h) HAp after 1 day of incubation. Abbreviations used are HAp microcarriers (HAp), DAT Coated HAp microcarriers (DAT-HAp), HAp microcarriers loaded with 0.01 mg/ml SIM (HAp-0.01), DAT coated HAp microcarriers loaded with 0.01 mg/ml SIM (DAT-HAp-0.01), HAp microcarriers loaded with 0.1 mg/ml SIM (HAp-0.1), DAT coated HAp microcarriers loaded with 0.1 mg/ml SIM (DAT-HAp-0.1), HAp microcarriers loaded with 0.5 mg/ml SIM (HAp-0.5), DAT coated HAp microcarriers loaded with 0.5 mg/ml SIM (DAT-HAp-0.5).

### 3.5.3. Laser Confocal Microscopy of Cell Seeded HAp based Microcarriers

SEM analyses revealed that the prepared microcarriers were porous; therefore the available surface for cell attachment was increased. The cell attachment on microcarriers was also confirmed with CLSM. In CLSM, non-specific FITC staining of HAp microcarriers was observed. Only nuclei of attached cells were stained (Figure 21). Cell growth on microcarriers was also observed in Z-stack analyses with CLSM (Figure 22). Since the nuclei of cells can be seen when the laser goes deeper, the cells surrounded the microcarriers showing that the cells attached and migrated homogenously on the surface of the microcarriers.

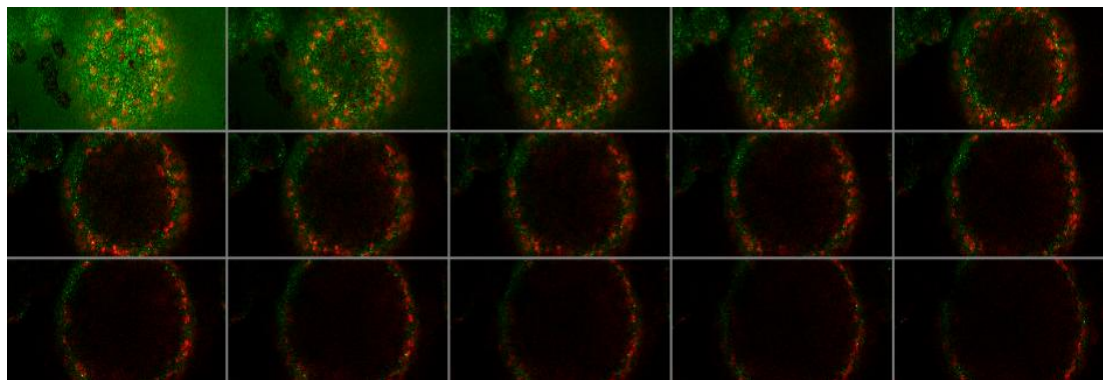


**Figure 21.** Z-stack images of cells attached on microcarriers after 24 hours of incubation.

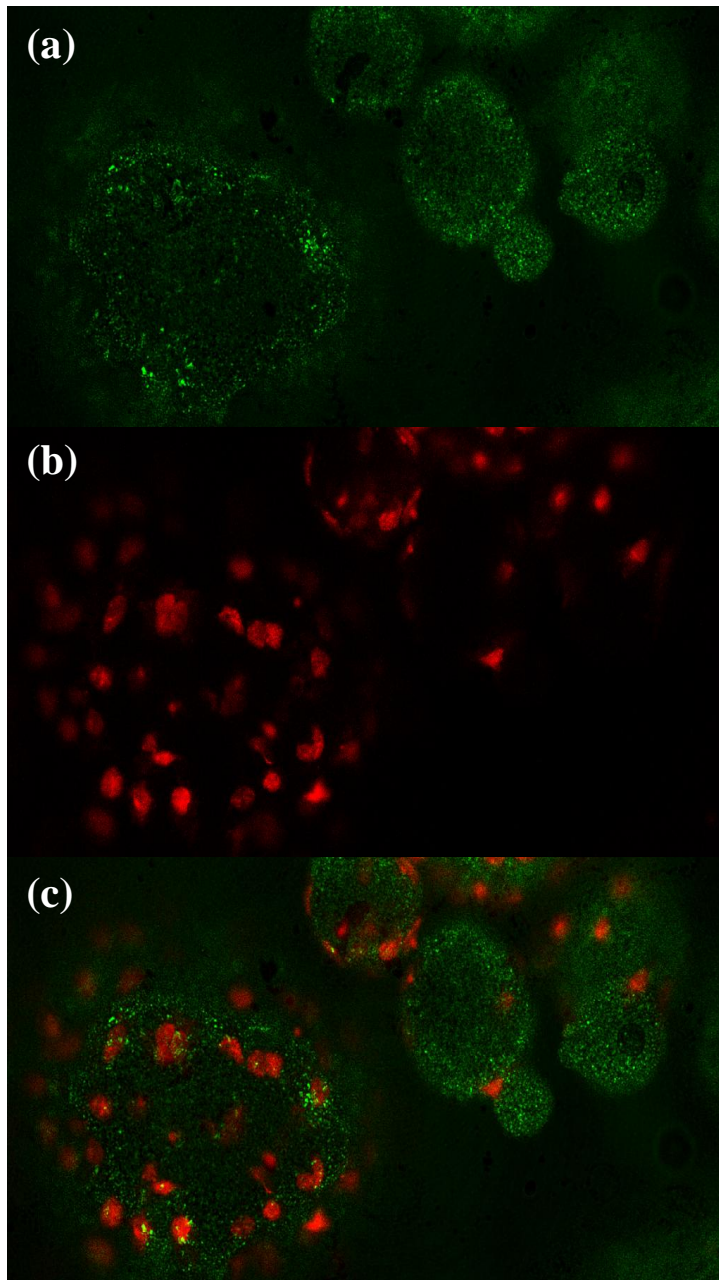


**Figure 22.** Z-stack images of microcarriers that were (a) non-specifically stained with FITC, (b) nuclei of Saos-2 cells stained with PI and (c) cells (stained with PI-red) attached on the microcarriers (stained with FITC-green).

### 3.5.4. Osteoblastic Differentiation of Saos-2 cells Seeded on HAp Based Microcarriers

Osteogenic differentiation of Saos-2 cells on SIM loaded HAp based DAT coated and uncoated microcarriers was conducted in osteogenic induction medium for 14 days. Detailed surface characterization was examined on day 7 by SEM and SEM-EDX spot analysis (**Figures 23** and **24**). According to SEM images, precipitated calcium phosphate particles were observed on the surfaces of cells that were attached onto microcarriers. Attached cell density on DAT coated microcarriers was observed to be higher than uncoated microcarriers. In order to see atomic ratio difference of Ca/P between DAT coated and uncoated microcarriers surface, SEM observations were supported with EDX spot analysis. Carbon (C) amounts shown in EDX graphs of DAT coated microcarriers were higher than uncoated HAp microcarriers. This can be attributed to organic compounds of DAT; however, the carbon content also differs in between each sample that were coated with DAT. It can be due to attached cell density difference. In **Figure 23 (a)**, carbon amount of DAT-HAp-0.5 were lowest among DAT-coated group. In viability studies, we have seen that when SIM concentration in microcarriers was lowered, attached cell density was shown to be increased. Therefore, it can be said that SIM concentration in DAT-HAp-0.5 decreased the cell attachment with respect to other DAT-coated microcarriers. Semiquantitative analysis of Ca/P ratios can be used to indicate the phase of Ca-P present on the cell layer with SEM-EDX (Lickorish et al., 2004). Average Ca/P atomic ratio determined according to coating difference by EDX analysis. Data were collected from top of the cell layers on DAT coated and uncoated microcarriers groups were averaged for (HAp and DAT-HAp microcarriers)  $1.65 \pm 0.08$  and  $1.44 \pm 0.29$ , respectively. Compared to stoichiometric HAp (Ca/P=1.67), uncoated microcarriers were shown to have lower than stoichiometric HAp ratio and was closer to Ca-deficient hydroxyapatite (Ca/P~1.5) (N. Zhang et al., 2013). However, microcarriers were HAp microsphere as it has been shown from the XRD analyses of starting powders and calcined microcarriers (**Figure 5** and **6**) and EDX analysis did

not provide enough data for deciding the effect of SIM on cell differentiation. It must be supported SEM and ALP specific enzyme activity analyses.

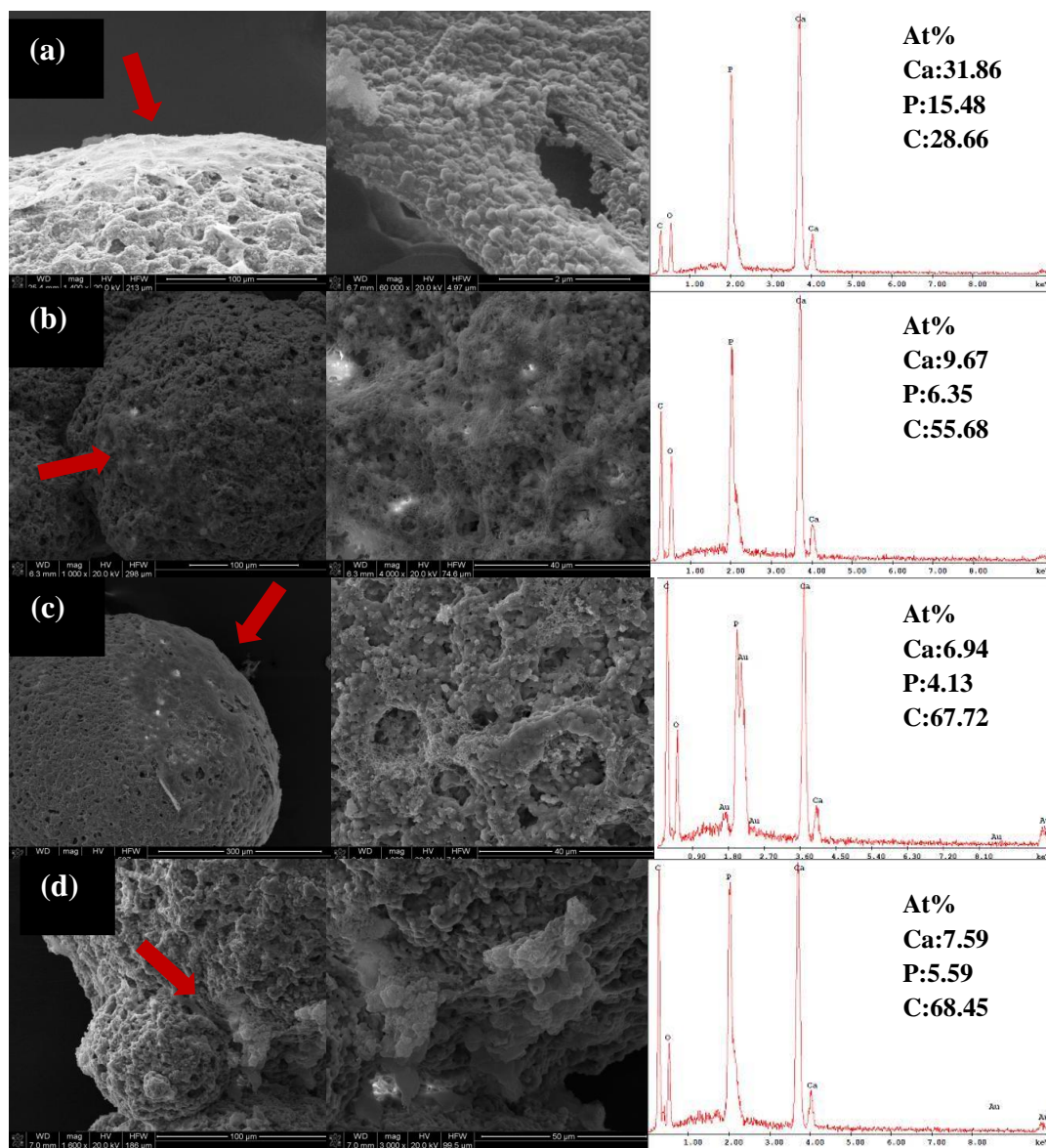


**Figure 23.** SEM images and EDX-SEM analysis results of Saos-2 seeded on (a) DAT-HAp-0.5 (b) DAT-HAp-0.1 (c) DAT-HAp-0.01 (d) DAT-HAp after 7 days of incubation in osteogenic media. Spotted areas for EDX analysis were shown by arrows.

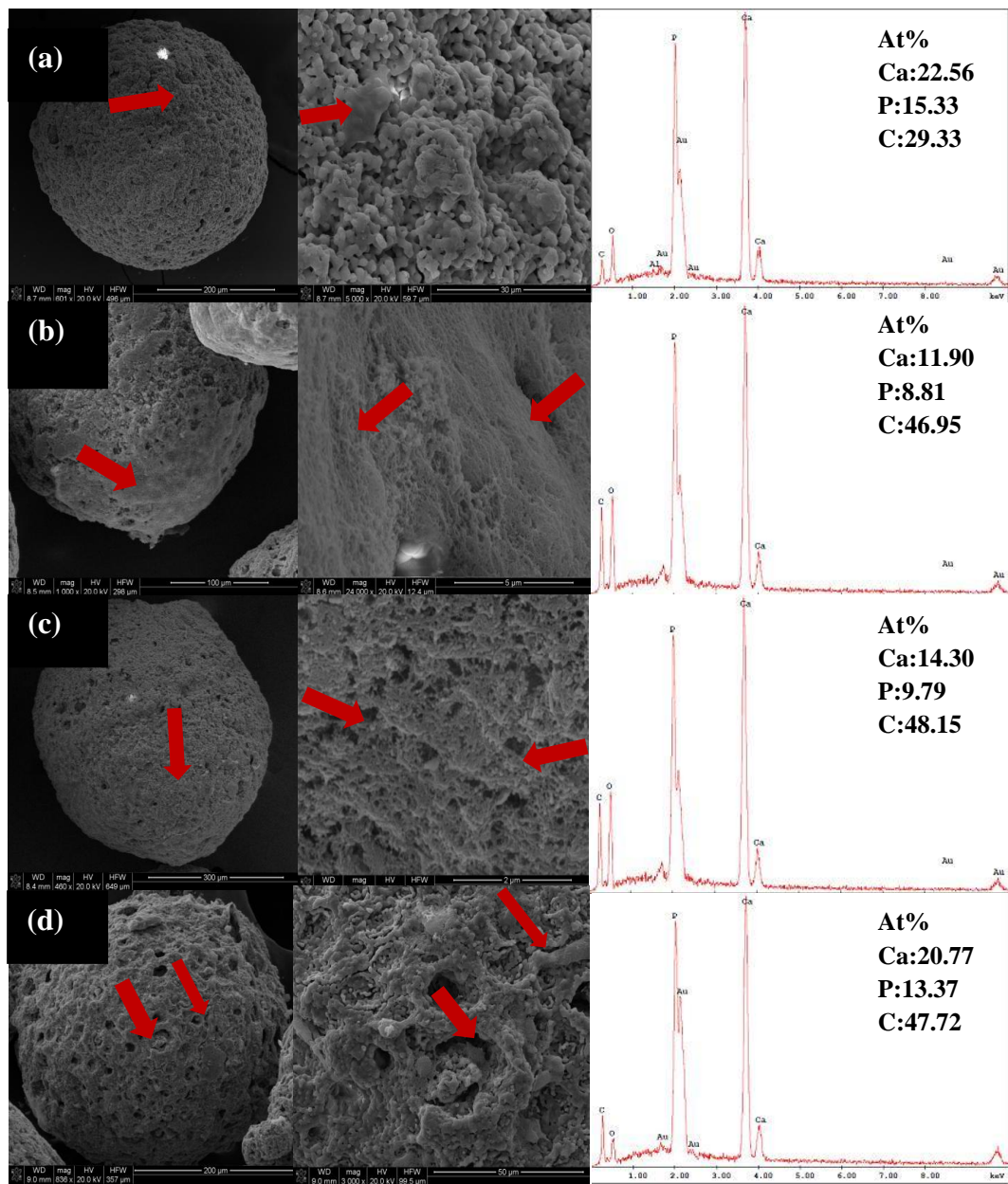


**Figure 24.** SEM images and EDX-SEM spot analysis of Saos-2 seeded on (a) HAp-0.5 (b) HAp-0.1 (c) HAp-0.01 (d) HAp after 7<sup>th</sup> day of incubation in osteogenic induction media. Spotted areas for EDX analysis were shown by arrows.



## CHAPTER 4

### CONCLUSIONS

Spherical microparticles have been widely used form of biomaterials, generally used for cell and drug delivery purposes in tissue engineering applications. In this study, porous hydroxyapatite based microcarriers were formed by w/o emulsification method and loaded with 0.01, 0.1, 0.5 mg/ml simvastatin, respectively. Coated with decellularized adipose tissue increased cellular attachment and proliferation on the microcarriers. Although, the loaded amount of SIM was determined in cytotoxic level in literature, microcarriers were not shown to be cytotoxic on both saos-2 cells and human adipose-derived stem cells. *In vitro* experiments suggest that SIM loaded and DAT coated microcarriers can be applied to improve osteogenic activity and regeneration at the defect site. However, firstly, SIM loaded and coated microcarriers long term effect should be evaluated *in vivo*.



## REFERENCES

- Albrektsson, T., & Johansson, C. (2001). Osteoinduction, osteoconduction and osseointegration. *European Spine Journal: Official Publication of the European Spine Society, the European Spinal Deformity Society, and the European Section of the Cervical Spine Research Society*, 10(2), 96–101.
- Amsa, P., Tamizharasi, S., Jagadeeswaran, M., & Sivakumar, T. (2014). Preparation and Solid State Characterization of Simvastatin Nanosuspensions for Enhanced Solubility and Dissolution. *International Journal of Pharmacy and Pharmaceutical Sciences*, 6(1), 2–6.
- Araki, K., & Halloran, J. W. (2005). Porous Ceramic Bodies with Interconnected Pore Channels by a Novel Freeze Casting Technique. *Journal of the American Ceramic Society*, 88(5), 1108–1114.
- Arnett T. (2003). Regulation of bone cell function by acid-base balance. *Proc Nutr Soc* 62: 511–520.
- Badylak, S. F., Taylor, D., & Uygun, K. (2011). Whole-organ tissue engineering: decellularization and recellularization of three-dimensional matrix scaffolds. *Annual Review of Biomedical Engineering*, 13, 27–53.
- Barrias, C. C., Ribeiro, C. C., Lamghari, M., Miranda, C. S., & Barbosa, M. a. (2005). Proliferation, activity, and osteogenic differentiation of bone marrow stromal cells cultured on calcium titanium phosphate microspheres. *Journal of Biomedical Materials Research. Part A*, 72(1), 57–66.
- Benders, K. E. M., van Weeren, P. R., Badylak, S. F., Saris, D. B. F., Dhert, W. J. A., & Malda, J. (2013). Extracellular matrix scaffolds for cartilage and bone regeneration. *Trends in Biotechnology*, 31(3), 169–76.
- Bianco, P., & Robey, P. G. (2001). Stem cells in tissue engineering. *Nature*, 414(6859), 118–21.
- Bohner, M., Tadier, S., Van Garderen, N., de Gasparo, A., Döbelin, N., & Baroud, G. (2013). Synthesis of spherical calcium phosphate particles for dental and orthopedic applications. *Biomatter*, 3(2), 1–15.

- Buchanan, R. a, Lee, I. S., & Williams, J. M. (1990). Surface modification of biomaterials through noble metal ion implantation. *Journal of Biomedical Materials Research*, 24(3), 309–18.
- Bunnell, B. a, Flaat, M., Gagliardi, C., Patel, B., & Ripoll, C. (2008). Adipose-derived stem cells: isolation, expansion and differentiation. *Methods (San Diego, Calif.)*, 45(2), 115–20.
- Cai, Y., Liu, Y., Yan, W., Hu, Q., Tao, J., Zhang, M., Tang, R. (2007). Role of hydroxyapatite nanoparticle size in bone cell proliferation. *Journal of Materials Chemistry*, 17(36), 3780.
- Champion, E. (2013). Sintering of calcium phosphate bioceramics. *Acta Biomaterialia*, 9(4), 5855–75.
- Cheifetz, S., Li, I. W., McCulloch, C. A., Sampath, K., & Sodek, J. (1996). Influence of osteogenic protein-1 (OP-1;BMP-7) and transforming growth factor-beta 1 on bone formation in vitro. *Connective Tissue Research*, 35(1-4), 71–8.
- Chen, T. L., Shen, W. J., & Kraemer, F. B. (2001). Human BMP-7/OP-1 induces the growth and differentiation of adipocytes and osteoblasts in bone marrow stromal cell cultures. *Journal of Cellular Biochemistry*, 82(2), 187–99.
- Cheng, C. W., Solorio, L. D., & Alsberg, E. (2014). Decellularized tissue and cell-derived extracellular matrices as scaffolds for orthopaedic tissue engineering. *Biotechnology Advances*, 32(2), 462–84.
- Chou, J., Ito, T., Bishop, D., Otsuka, M., Ben-Nissan, B., & Milthorpe, B. (2013). Controlled release of simvastatin from biomimetic  $\beta$ -TCP drug delivery system. *PloS One*, 8(1), e54676.
- Cinotti, G., Corsi, A., Sacchetti, B., Riminucci, M., Bianco, P., & Giannicola, G. (2013). Bone ingrowth and vascular supply in experimental spinal fusion with platelet-rich plasma. *Spine*, 38(5), 385–91.
- Clarke, B. (2008). Normal bone anatomy and physiology. *Clinical Journal of the American Society of Nephrology : CJASN*, 3 Suppl 3, S131–9.
- Crockett, J. C., Rogers, M. J., Coxon, F. P., Hocking, L. J., & Helfrich, M. H. (2011). Bone remodelling at a glance. *Journal of Cell Science*, 124(Pt 7), 991–8.

- Damaraju S. and Duncan, N.A. (2014) Stem cell-based tissue engineering for bone repair: influence of cell communication and 3-D cell-matrix environment. *Tissue Engineering: Computer Modeling, Biofabrication and Cell Behavior*, PR and Bartolo, PJ. In: *Computational Methods in Applied Sciences*, (Eds. Fernandes, Vol. 31, pp. 1-31). Springer.
- Dimitriou, R., Jones, E., McGonagle, D., & Giannoudis, P. V. (2011). Bone regeneration: current concepts and future directions. *BMC Medicine*, 9(1), 66.
- Dimitriou, R., Tsiridis, E., & Giannoudis, P. V. (2005). Current concepts of molecular aspects of bone healing. *Injury*, 36(12), 1392–404.
- Diramio, J. A., Kisaalita, W. S., Majetich, G. F., & Shimkus, J. M. (2008). Poly(ethylene glycol) methacrylate/dimethacrylate hydrogels for controlled release of hydrophobic drugs. *Biotechnology Progress*, 21(4), 1281–8.
- Dorozhkin, S. V. (2010). Nanosized and nanocrystalline calcium orthophosphates. *Acta Biomaterialia*, 6(3), 715–34.
- Dupoirieux, L., Pourquier, D., Picot, M. C., & Neves, M. (2001). Comparative study of three different membranes for guided bone regeneration of rat cranial defects. *International Journal of Oral and Maxillofacial Surgery*, 30(1), 58–62.
- Eom, Y. W., Lee, J. E., Yang, M. S., Jang, I. K., Kim, H. E., Lee, D. H., Kim, H. S. (2011). Rapid isolation of adipose tissue-derived stem cells by the storage of lipoaspirates. *Yonsei Medical Journal*, 52(6), 999–1007.
- Eriksen, E. F. (2010). Cellular mechanisms of bone remodeling. *Reviews in Endocrine & Metabolic Disorders*, 11(4), 219–27.
- Fadli, A., Sopyan, I., Mel, M., & Ahmad, Z. (2011). Porous alumina through protein foaming – consolidation method: effect of dispersant concentration on the physical. *Asia-Pacific Journal of Chemical Engineering*, 6(6), 863-869
- Fazio, S., Guzmán, J., Colomer, M. T., Salomoni, a., & Moreno, R. (2008). Colloidal stability of nanosized titania aqueous suspensions. *Journal of the European Ceramic Society*, 28(11), 2171–2176.
- Fiedler, J., Gu, K., Puhl, W., & Kessler, S. (2001). Proliferation and differentiation rates of a human osteoblast-like cell line ( SaOS-2 ) in contact with different bone substitute materials. *J Biomed Mater Res.*, 57(1),132-9

- Flynn, L., Semple, J. L., & Woodhouse, K. A. (2006). Decellularized placental matrices for adipose tissue engineering. *Journal of Biomedical Materials Research. Part A*, 79(2), 359–69.
- Francis, L., Meng, D., Knowles, J., Keshavarz, T., Boccaccini, A. R., & Roy, I. (2011). Controlled delivery of gentamicin using poly(3-hydroxybutyrate) microspheres. *International Journal of Molecular Sciences*, 12(7), 4294–314.
- Gibson, M., Beachley, V., Coburn, J., Bandinelli, P. A., Mao, H.-Q., & Elisseff, J. (2014). Tissue Extracellular Matrix Nanoparticle Presentation in Electrospun Nanofibers. *BioMed Research International*, 2014, 1–13.
- Goad, D. L., Rubin, J., Wang, H., Tashjian, A. H., & Patterson, C. (1996). Enhanced expression of vascular endothelial growth factor in human SaOS-2 osteoblast-like cells and murine osteoblasts induced by insulin-like growth factor I. *Endocrinology*, 137(6), 2262–8.
- Goh, T. K.-P., Zhang, Z.-Y., Chen, A. K.-L., Reuveny, S., Choolani, M., Chan, J. K. Y., & Oh, S. K.-W. (2013). Microcarrier culture for efficient expansion and osteogenic differentiation of human fetal mesenchymal stem cells. *BioResearch Open Access*, 2(2), 84–97.
- Gray IV RW, Baird DG, B. J. (1998). Effects of processing conditions on short TCLP fiber reinforced FDM parts. *Rapid Prototyping Journal*, 4(1), 14–25.
- Groeneveld, E., & Burger, E. (2000). Bone morphogenetic proteins in human bone regeneration. *European Journal of Endocrinology*, 142(1), 9–21.
- Gutierrez, G. E., Edwards, J. R., Garrett, I. R., Nyman, J. S., McCluskey, B., Rossini, G., Mundy, G. R. (2008). Transdermal lovastatin enhances fracture repair in rats. *Journal of Bone and Mineral Research: The Official Journal of the American Society for Bone and Mineral Research*, 23(11), 1722–30.
- Hong, M.-H., Son, J.-S., Kim, K.-M., Han, M., Oh, D. S., & Lee, Y.-K. (2011). Drug-loaded porous spherical hydroxyapatite granules for bone regeneration. *Journal of Materials Science. Materials in Medicine*, 22(2), 349–55.
- Hong, S.-J., Yu, H.-S., & Kim, H.-W. (2009). Preparation of porous bioactive ceramic microspheres and in vitro osteoblastic culturing for tissue engineering application. *Acta Biomaterialia*, 5(5), 1725–31.
- Hong, S.-J., Yu, H.-S., & Kim, H.-W. (2009). Tissue engineering polymeric microcarriers with macroporous morphology and bone-bioactive surface. *Macromolecular Bioscience*, 9(7), 639–45.

- Hopkins, R. A., Bert, A. A., Hilbert, S. L., Quinn, R. W., Brasky, K. M., Drake, W. B., & Lofland, G. K. (2013). Bioengineered human and allogeneic pulmonary valve conduits chronically implanted orthotopically in baboons: hemodynamic performance and immunologic consequences. *The Journal of Thoracic and Cardiovascular Surgery*, *145*(4), 1098–107.
- Hoshiba, T., Lu, H., Kawazoe, N., & Chen, G. (2010). Decellularized matrices for tissue engineering. *Expert Opinion on Biological Therapy*, *10*(12), 1717–28.
- Hu, J., Liu, X., & Ma, P. X. (2011). Bone Regeneration. In: *Principles of Regenerative Medicine* (Second Ed., pp. 733–745). Elsevier Inc.
- Im, G.-I., Shin, Y.-W., & Lee, K.-B. (2005). Do adipose tissue-derived mesenchymal stem cells have the same osteogenic and chondrogenic potential as bone marrow-derived cells? *Osteoarthritis and Cartilage / OARS, Osteoarthritis Research Society*, *13*(10), 845–53.
- Jaiswal, R. K., Jaiswal, N., Bruder, S. P., Mbalaviele, G., Marshak, D. R., & Pittenger, M. F. (2000). Adult human mesenchymal stem cell differentiation to the osteogenic or adipogenic lineage is regulated by mitogen-activated protein kinase. *The Journal of Biological Chemistry*, *275*(13), 9645–52.
- Jeong, I., Yu, H.-S., Kim, M.-K., Jang, J.-H., & Kim, H.-W. (2010). FGF2-adsorbed macroporous hydroxyapatite bone granules stimulate in vitro osteoblastic gene expression and differentiation. *Journal of Materials Science. Materials in Medicine*, *21*(4), 1335–42.
- Johari, N., Fathi, M. H., & Golozar, M. a. (2012). Fabrication, characterization and evaluation of the mechanical properties of poly ( $\epsilon$ -caprolactone)/nano-fluoridated hydroxyapatite scaffold for bone tissue engineering. *Composites Part B: Engineering*, *43*(3), 1671–1675.
- Kakudo, N., Minakata, T., Mitsui, T., Kushida, S., Notodihardjo, F. Z., & Kusumoto, K. (2008). Proliferation-promoting effect of platelet-rich plasma on human adipose-derived stem cells and human dermal fibroblasts. *Plastic and Reconstructive Surgery*, *122*(5), 1352–60.
- Kehoe, D. E., Jing, D., Lock, L. T., Tzanakakis, E. S., & Ph, D. (2010). Scalable Stirred-Suspension Bioreactor Culture, *16*(2), 405-421.
- Kellomäki, M., Niiranen, H., Puumanen, K., Ashammakhi, N., Waris, T., & Törmälä, P. (2000). Bioabsorbable scaffolds for guided bone regeneration and generation. *Biomaterials*, *21*(24), 2495–505.

- Kolar, P., Gaber, T., Perka, C., Duda, G. N., & Buttgerit, F. (2011). Human early fracture hematoma is characterized by inflammation and hypoxia. *Clinical Orthopaedics and Related Research*, 469(11), 3118–26.
- Lee, E.-J., Koh, Y.-H., Yoon, B.-H., Kim, H.-E., & Kim, H.-W. (2007). Highly porous hydroxyapatite bioceramics with interconnected pore channels using camphene-based freeze casting. *Materials Letters*, 61(11-12), 2270–2273.
- Li, B., Guo, B., Fan, H., & Zhang, X. (2008). Preparation of nano-hydroxyapatite particles with different morphology and their response to highly malignant melanoma cells in vitro. *Applied Surface Science*, 255(2), 357–360.
- Lickorish, D., Ramshaw, J. A. M., Werkmeister, J. A., Glattauer, V., & Howlett, C. R. (2004). Collagen-hydroxyapatite composite prepared by biomimetic process. *Journal of Biomedical Materials Research. Part A*, 68(1), 19–27.
- Lieberman, J. R., Daluiski, A., & Einhorn, T. A. (2002). The Role of Growth Factors in the Repair of Bone. *The Journal of Bone and Joint Surgery.*, 84, 1032–1044.
- Lin, Z.-Y., Duan, Z.-X., Guo, X.-D., Li, J.-F., Lu, H.-W., Zheng, Q.-X., Yang, S.-H. (2010). Bone induction by biomimetic PLGA-(PEG-ASP)<sub>n</sub> copolymer loaded with a novel synthetic BMP-2-related peptide in vitro and in vivo. *Journal of Controlled Release : Official Journal of the Controlled Release Society*, 144(2), 190–5.
- Lupattelli, G., Scarponi, A. M., Vaudo, G., Siepi, D., Roscini, A. R., Gemelli, F., Mannarino, E. (2004). Simvastatin increases bone mineral density in hypercholesterolemic postmenopausal women. *Metabolism: Clinical and Experimental*, 53(6), 744–8.
- Zhou, W., & Ma, G. (2013). Microspheres for Cell Culture. In: *Microspheres and Microcapsules in Biotechnology* (pp. 49–83). Pan Stanford Publishing.
- Malda, J., van Blitterswijk, C. A., Grojec, M., Martens, D. E., Tramper, J., & Riesle, J. (2003). Expansion of bovine chondrocytes on microcarriers enhances redifferentiation. *Tissue Engineering*, 9(5), 939–48.
- Mason, C. (2005). Tissue engineering skin: a paradigm shift in wound care. *Medical Device Technology*, 16(10), 32–3.
- M.C. Farach-Carson, R.C. Wagner, and K.L. Kiick (2007). Extracellular Matrix: Structure, Function, and Applications to Tissue Engineering Fisher, J. P., Mikos, A. G., & Bronzino, J. D. In: *Tissue Engineering*. CRC press.

- Meinel, L., Illi, O. E., Zapf, J., Malfanti, M., Peter Merkle, H., & Gander, B. (2001). Stabilizing insulin-like growth factor-I in poly(D,L-lactide-co-glycolide) microspheres. *Journal of Controlled Release : Official Journal of the Controlled Release Society*, 70(1-2), 193–202.
- Mistry, A. S., & Mikos, A. G. (2005). Tissue Engineering Strategies for Bone Regeneration, 94, 1–22.
- Mundy, G. (1999). Stimulation of Bone Formation in Vitro and in Rodents by Statins. *Science*, 286(5446), 1946–1949.
- Mundy, G. R. (2000). Pathogenesis of osteoporosis and challenges for drug delivery. *Advanced Drug Delivery Reviews*, 42(3), 165–73.
- Murugan, R., & Ramakrishna, S. (2005). Development of nanocomposites for bone grafting. *Composites Science and Technology*, 65, 2385–2406.
- Nerem, R. M. (2007). Two The Challenge of Imitating Nature. In R. Lanza, R. Langer, & J. Vacanti, *Principles of Tissue Engineering* (3th ed., pp. 7–14). Academic Press.
- Nikolidakis, D., & Jansen, J. a. (2008). The biology of platelet-rich plasma and its application in oral surgery: literature review. *Tissue Engineering. Part B, Reviews*, 14(3), 249–58. doi:10.1089/ten.teb.2008.0062
- Nissan, B. (2014). Advances in Calcium Phosphate Nanocoatings and Nanocomposites. In *Advances in calcium phosphate biomaterials* (Besim ed., Vol. 2, pp. 485-509). Berlin: Wiley.
- Ogawa, R., Mizuno, H., Watanabe, A., Migita, M., Shimada, T., & Hyakusoku, H. (2004). Osteogenic and chondrogenic differentiation by adipose-derived stem cells harvested from GFP transgenic mice. *Biochemical and Biophysical Research Communications*, 313(4), 871–877. doi:10.1016/j.bbrc.2003.12.017
- Okuda, K., Kawase, T., Momose, M., Murata, M., Saito, Y., Suzuki, H., Yoshie, H. (2003). Platelet-Rich Plasma Contains High Levels of Platelet-Derived Growth Factor- $\beta$  and Modulates the Proliferation of Perodontally Related Cells In Vitro. *Journal of Periodontol*, 74(6), 849–857.
- Oliveira, M. B., & Mano, J. F. (2011). Polymer-based microparticles in tissue engineering and regenerative medicine. *Biotechnology Progress*.

- Park, B.-W., Kang, E.-J., Byun, J.-H., Son, M.-G., Kim, H.-J., Hah, Y.-S., Rho, G.-J. (2012). In vitro and in vivo osteogenesis of human mesenchymal stem cells derived from skin, bone marrow and dental follicle tissues. *Differentiation; Research in Biological Diversity*, 83(5), 249–59.
- Park, J. (2008). Structure of Ceramic and Glasses. In: *Bioceramics*. J. Park, pp 364 . Springer.
- Park, J. (2012). Microcarriers designed for cell culture and tissue engineering of bone. *Tissue Engineering Part B: Reviews*, 1–53.
- Park, J., & Lakes, R. S. (2007). *Biomaterials: An Introduction* (p. 576). Springer.
- Park, J., & Pe, A. (2013). Microcarriers Designed for Cell Culture and Tissue Engineering of Bone, *19*(2).
- Partridge, K., Yang, X., Clarke, N. M. P., Okubo, Y., Bessho, K., Sebald, W., Oreffo, R. O. C. (2002). Adenoviral BMP-2 Gene Transfer in Mesenchymal Stem Cells: In Vitro and in Vivo Bone Formation on Biodegradable Polymer Scaffolds. *Biochemical and Biophysical Research Communications*, 292(1), 144–152.
- Pati, F., Jang, J., Ha, D.-H., Won Kim, S., Rhie, J.-W., Shim, J.-H., Cho, D.-W. (2014). Printing three-dimensional tissue analogues with decellularized extracellular matrix bioink. *Nature Communications*, 5, 3935.
- Pattanayak, D. K., Rao, B. T., & Mohan, T. R. R. (2010). Calcium phosphate bioceramics and bioceramic composites. *Journal of Sol-Gel Science and Technology*, 59(3), 432–447.
- Pittenger, M. F. (1999). Multilineage Potential of Adult Human Mesenchymal Stem Cells. *Science*, 284(5411), 143–147.
- Pritchard, J. J. (1972). General Histology of Bone. G. H. Bourne In, *The Biochemistry and Physiology of Bone* (pp. 1–19). New York and London: Academic Press.
- Ravaglio, A., & Krajewski, A. (1992). *Bioceramics*. (S. F. Hulbert, Ed.). London: Chapman&Hall.
- Reddi, A. H. (2001). Bone morphogenetic proteins: from basic science to clinical applications. *The Journal of Bone and Joint Surgery. American Volume*, 83(1), 1–6.

- Rizzi, S. C., Heath, D. J., Coombes, a G., Bock, N., Textor, M., & Downes, S. (2001). Biodegradable polymer/hydroxyapatite composites: surface analysis and initial attachment of human osteoblasts. *Journal of Biomedical Materials Research*, 55(4), 475–86.
- Roberts, A. D., & Zhang, H. (2013). Poorly water-soluble drug nanoparticles via solvent evaporation in water-soluble porous polymers. *International Journal of Pharmaceutics*, 447(1-2), 241–50.
- Rojbani, H., Nyan, M., Ohya, K., & Kasugai, S. (2011). Evaluation of the osteoconductivity of  $\alpha$ -tricalcium phosphate,  $\beta$ -tricalcium phosphate, and hydroxyapatite combined with or without simvastatin in rat calvarial defect. *Journal of Biomedical Materials Research. Part A*, 98(4), 488–98.
- Sadat-Shojai, M., Khorasani, M.-T., Dinpanah-Khoshdargi, E., & Jamshidi, A. (2013). Synthesis methods for nanosized hydroxyapatite with diverse structures. *Acta Biomaterialia*, 9(8), 7591–621.
- Safford, K. M., Safford, S. D., Gimble, J. M., Shetty, A. K., & Rice, H. E. (2004). Characterization of neuronal/glial differentiation of murine adipose-derived adult stromal cells. *Experimental Neurology*, 187(2), 319–28.
- Salgado, A. J., Coutinho, O. P., & Reis, R. L. (2004). Bone tissue engineering: state of the art and future trends. *Macromolecular Bioscience*, 4(8), 743–65.
- Salinas, A. J., Esbrit, P., & Vallet-Regí, M. (2013). A tissue engineering approach based on the use of bioceramics for bone repair. *Biomaterials Science*, 1(1), 40.
- Sanosh, K. P., Chu, M.-C., Balakrishnan, a., Kim, T. N., & Cho, S.-J. (2009). Preparation and characterization of nano-hydroxyapatite powder using sol-gel technique. *Bulletin of Materials Science*, 32(5), 465–470.
- Santoni, B. G., Pluhar, G. E., Motta, T., & Wheeler, D. L. (2007). Hollow calcium phosphate microcarriers for bone regeneration: in vitro osteoproduction and ex vivo mechanical assessment. *Bio-Medical Materials and Engineering*, 17(5), 277–89.
- Serajuddin, A. T., Ranadive, S. A., & Mahoney, E. M. (1991). Relative lipophilicities, solubilities, and structure-pharmacological considerations of 3-hydroxy-3-methylglutaryl-coenzyme A (HMG-CoA) reductase inhibitors pravastatin, lovastatin, mevastatin, and simvastatin. *Journal of Pharmaceutical Sciences*, 80(9), 830–4.

- Shi, Y., Niedzinski, J. R., Samaniego, A., Bogdansky, S., & Atkinson, B. L. (2012). Adipose-derived stem cells combined with a demineralized cancellous bone substrate for bone regeneration. *Tissue Engineering. Part A*, 18(13-14), 1313–21.
- Silva, G. A., Coutinho, O. P., Ducheyne, P., & Reis, R. L. (2007). Materials in particulate form for tissue engineering . 2 . Applications in bone, (March), 97–109.
- Simsek, D. (2002). *Preparation and Characterization of HA Powders - Dense and Porous HA Based Composite Materials, A Dissertation* Submitted to the Department : Materials Science and Engineering. Izmir Institute of Technology.
- Song, C., Guo, Z., Ma, Q., Chen, Z., Liu, Z., Jia, H., & Dang, G. (2003). Simvastatin induces osteoblastic differentiation and inhibits adipocytic differentiation in mouse bone marrow stromal cells. *Biochemical and Biophysical Research Communications*, 308(3), 458–462.
- Sottile, V., Thomson, A., & McWhir, J. (2003). In vitro osteogenic differentiation of human ES cells. *Cloning and Stem Cells*, 5(2), 149–55.
- Stein, D., Lee, Y., Schmid, M. J., Killpack, B., Genrich, M. A., Narayana, N., Reinhardt, R. A. (2006). NIH Public Access, 76(11), 1861–1870.
- Strem, B. M., Hicok, K. C., Zhu, M., Wulur, I., Alfonso, Z., Schreiber, R. E., Hedrick, M. H. (2005). Multipotential differentiation of adipose tissue-derived stem cells. *The Keio Journal of Medicine*, 54(3), 132–41.
- Tanner, K. E. (2010). Bioactive composites for bone tissue engineering. *Proceedings of the Institution of Mechanical Engineers , Part H : Journal of Engineering in Medicine*, 224(12), 1359-1372.
- Teng, S., & Chen, L. (2007). Formation of nano-hydroxyapatite in gelatin droplets and the resulting porous composite microspheres, 101, 686–691.
- Tezcaner, A., & Keskin, D. (2011). Bioactive Agent Delivery in Bone Tissue Regeneration. In J. I. et Al. (Ed.), *Stud. Mechanobiol. Tissue Eng. Biomater.* (pp. 193–223). Springer.
- Turner, A. E. B., Yu, C., Bianco, J., Watkins, J. F., & Flynn, L. E. (2012). The performance of decellularized adipose tissue microcarriers as an inductive substrate for human adipose-derived stem cells. *Biomaterials*, 33(18), 4490–9.

- Upton, J., & Glowacki, J. (1992). Hand reconstruction with allograft demineralized bone: Twenty-six implants in twelve patients. *Journal of Hand Surgery*, 17(4), 704–713.
- Uter, L. (2006). Tissue Specific Stem Cells Comparative Analysis of Mesenchymal Stem Cells from Bone Marrow , Umbilical Cord Blood , or Adipose Tissue,24, 1294–1301.
- Valletregi, M. (2004). Calcium phosphates as substitution of bone tissues. *Progress in Solid State Chemistry*, 32(1-2), 1–31.
- Van, G. S., Kruyt, M., Meijer, G., Mistry, A., Mikos, A. G., van den Beucken, J., Dhert, W. (2008). Tissue Engineering of Bone. In C. Van Blitterswijk (Ed.), *Tissue Engineering* (first edit., pp. 559–611).
- Vats, a, Tolley, N. S., Polak, J. M., & Gough, J. E. (2003). Scaffolds and biomaterials for tissue engineering: a review of clinical applications. *Clinical Otolaryngology and Allied Sciences*, 28(3), 165–72.
- Wada, Y., Kataoka, H., Yokose, S., Ishizuya, T., Miyazono, K., Gao, Y. H., Yamaguchi, A. (1998). Changes in osteoblast phenotype during differentiation of enzymatically isolated rat calvaria cells. *Bone*, 22(5), 479–85.
- Wang, L., & Nancollas, G. H. (2009). Pathways to biomineralization and biodemineralization of calcium phosphates: the thermodynamic and kinetic controls. *Dalton Transactions (Cambridge, England : 2003)*, (15), 2665–72.
- Wang, Y., Liu, L., & Guo, S. (2010). Characterization of biodegradable and cytocompatible nano-hydroxyapatite/polycaprolactone porous scaffolds in degradation in vitro. *Polymer Degradation and Stability*, 95(2), 207–213.
- Webster, T. (2001). Enhanced osteoclast-like cell functions on nanophase ceramics. *Biomaterials*, 22(11), 1327–1333.
- Wei, G., & Ma, P. X. (2004). Structure and properties of nano-hydroxyapatite/polymer composite scaffolds for bone tissue engineering. *Biomaterials*, 25(19), 4749–57.
- Wozney, J. M., & Rosen, V. (1998). Bone morphogenetic protein and bone morphogenetic protein gene family in bone formation and repair. *Clinical Orthopaedics and Related Research*, (346), 26–37.

- Wu, C., Sun, X., Zhao, Z., Zhao, Y., Hao, Y., Liu, Y., & Gao, Y. (2014). Synthesis of novel core-shell structured dual-mesoporous silica nanospheres and their application for enhancing the dissolution rate of poorly water-soluble drugs. *Materials Science & Engineering. C, Materials for Biological Applications*, 44, 262–7.
- Yang, J.-H., Kim, K.-H., You, C.-K., Rautray, T. R., & Kwon, T.-Y. (2011). Synthesis of spherical hydroxyapatite granules with interconnected pore channels using camphene emulsion. *Journal of Biomedical Materials Research. Part B, Applied Biomaterials*, 99(1), 150–7.
- Yeh, L.-C. C., Adamo, M. L., Olson, M. S., & Lee, J. C. (2013). Osteogenic Protein-1 and Insulin-Like Growth Factor I Synergistically Stimulate Rat Osteoblastic Cell Differentiation and Proliferation. *Endocrinology*, 138(10).
- Yoon, B.-H., Koh, Y.-H., Park, C.-S., & Kim, H.-E. (2007). Generation of Large Pore Channels for Bone Tissue Engineering Using Camphene-Based Freeze Casting. *Journal of the American Ceramic Society*, 90(6), 1744–1752.
- Yoshimura, H., Muneta, T., Nimura, A., Yokoyama, A., Koga, H., & Sekiya, I. (2007). Comparison of rat mesenchymal stem cells derived from bone marrow, synovium, periosteum, adipose tissue, and muscle. *Cell and Tissue Research*, 327(3), 449–62.
- Young, D. A., Ibrahim, D. O., Hu, D., & Christman, K. L. (2011). Injectable hydrogel scaffold from decellularized human lipoaspirate. *Acta Biomaterialia*, 7(3), 1040–9.
- Zanetti, A. S., Sabliov, C., Gimble, J. M., & Hayes, D. J. (2013). Human adipose-derived stem cells and three-dimensional scaffold constructs: a review of the biomaterials and models currently used for bone regeneration. *Journal of Biomedical Materials Research. Part B, Applied Biomaterials*, 101(1), 187–99.
- Zang, M., Zhang, Q., Chang, E. I., Mathur, A. B., & Yu, P. (2012). Decellularized tracheal matrix scaffold for tissue engineering. *Plastic and Reconstructive Surgery*, 130(3), 532–40.
- Zhang, N., Molenda, J. a., Mankoci, S., Zhou, X., Murphy, W. L., & Sahai, N. (2013). Crystal structures of CaSiO<sub>3</sub> polymorphs control growth and osteogenic differentiation of human mesenchymal stem cells on bioceramic surfaces. *Biomaterials Science*, 1(10), 1101.

- Zhang, Y., Bradley, A. D., Wang, D., & Reinhardt, R. a. (2014). Statins, bone metabolism and treatment of bone catabolic diseases. *Pharmacological Research : The Official Journal of the Italian Pharmacological Society*, 1–9.
- Zhao, S., Wen, He F., Liu L., Yang G., (2014). In Vitro and In Vivo Evaluation of the Osteogenic Ability of Implant Surfaces with a Local Delivery of Simvastatin, *International Journal of Oral & Maxillofacial Implants*.29(1), 211–220.
- Zheng, L., Yang, F., Shen, H., Hu, X., Mochizuki, C., Sato, M., Zhang, Y. (2011). The effect of composition of calcium phosphate composite scaffolds on the formation of tooth tissue from human dental pulp stem cells. *Biomaterials*, 32(29), 7053–9.
- Zhou, Y., Ni, Y., Liu, Y., Zeng, B., Xu, Y., & Ge, W. (2010). The role of simvastatin in the osteogenesis of injectable tissue-engineered bone based on human adipose-derived stromal cells and platelet-rich plasma. *Biomaterials*, 31(20), 5325–35.



## APPENDIX A

### HPLC CALIBRATION CURVE

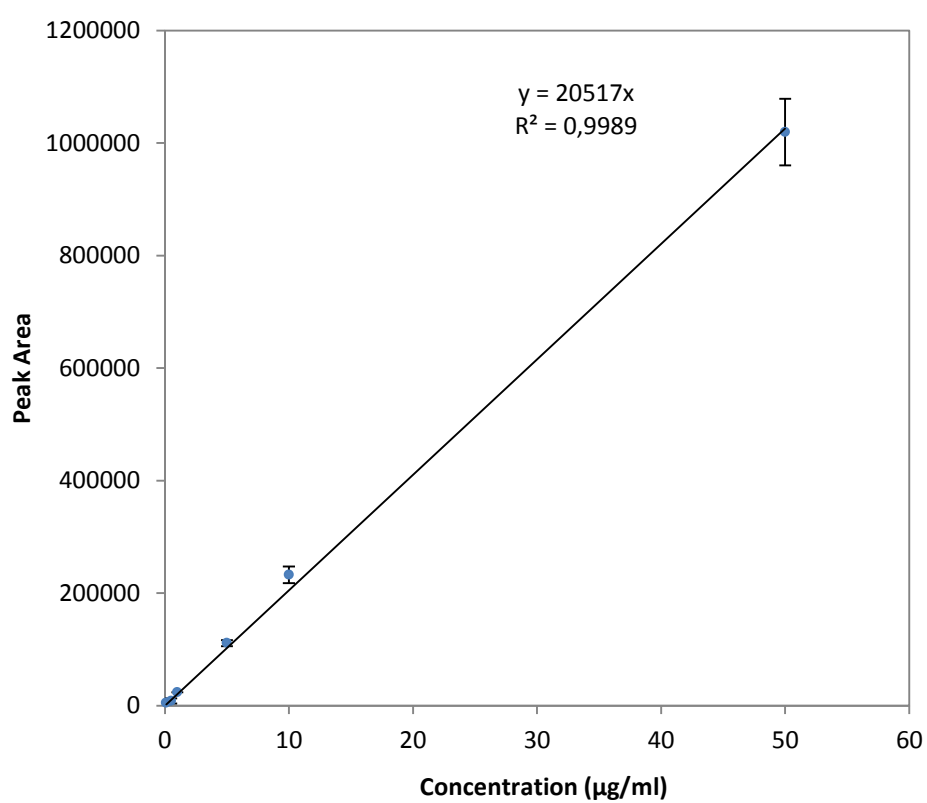


**Figure A1.** Calibration curve of SIM with HPLC UV-HPLC for determining drug amounts.



## APPENDIX B

### ETHICAL APPROVAL

UYGULAMALI ETİK ARAŞTIRMA MERKEZİ  
APPLIED ETHICS RESEARCH CENTER

 ORTA DOĞU TEKNİK ÜNİVERSİTESİ  
MIDDLE EAST TECHNICAL UNIVERSITY

DUMLUPINAR BULVARI 06800  
ÇANKAYA ANKARA/TURKEY  
T: +90 312 210 22 91  
F: +90 312 210 79 59  
ueam@metu.edu.tr  
www.ueam.metu.edu.tr

Sayı: 28620816/28 -130

15.01.2014

Gönderilen : Doç. Dr. Ayşen Tezcaner  
Mühendislik Bilimleri Bölümü

Gönderen : Prof. Dr. Canan Özgen  
IAK Başkanı



İlgi : Etik Onayı

Danışmanlığını yapmış olduğunuz Biyoteknoloji Bölümü öğrencisi Merve Güldiken "Kemik Hasarlarının Tedavisine Yönelik Simvastatin Yüklü Mikrotaşyıcıların Geliştirilmesi ve Karakterizasyonu" isimli araştırması "İnsan Araştırmaları Komitesi" tarafından uygun görülerek gerekli onay verilmiştir.

Bilgilerinize saygılarımla sunarım.

Etik Komite Onayı

Uygundur

15/01/2014



Prof. Dr. Canan Özgen  
Uygulamalı Etik Araştırma Merkezi  
(UEAM) Başkanı  
ODTÜ 06531 ANKARA

ODTÜ	
MÜHENDİSLİK FAKÜLTESİ DEKANLIĞI	
Yıl	Ay
2014	Ocak
1	2
3	4
5	6
7	8